Advances in Computational Mathematics (2019) 45:3265–3291
https://doi.org/10.1007/s10444-019-09737-2

Continuous interior penalty finite element methods for the time-harmonic Maxwell equation with high wave number

Peipei Lu[1] · **Haijun Wu**[2] · **Xuejun Xu**[3,4]

Received: 4 March 2019 / Accepted: 9 October 2019 /
Published online: 29 November 2019

Abstract

In this paper, using the first-order Nédélec conforming edge element space of the second type, we develop and analyze a continuous interior penalty finite element method (CIP-FEM) for the time-harmonic Maxwell equation in the three-dimensional space. Compared with the standard finite element methods, the novelty of the proposed method is that we penalize the jumps of the tangential component of its vorticity field. It is proved that if the penalty parameter is a complex number with negative imaginary part, then the CIP-FEM is well-posed without any mesh constraint. The error estimates for the CIP-FEM are derived. Numerical experiments are presented to verify our theoretical results.

Keywords Time-harmonic Maxwell equation · High wave number · Continuous interior penalty finite element method · Error estimates

Mathematics Subject Classification (2010) 65N12 · 65N15 · 65N30 · 78A40

Communicated by: Jan Hesthaven

✉ Peipei Lu
pplu@suda.edu.cn

Haijun Wu
hjw@nju.edu.cn

Xuejun Xu
xxj@lsec.cc.ac.cn

[1] School of Mathematics Sciences, Soochow University, Suzhou, 215006, China

[2] Department of Mathematics, Nanjing University, Jiangsu, 210093, China

[3] School of Mathematical Sciences, Tongji University, Shanghai, 200442, China

[4] LSEC, Institute of Computational Mathematics and Scientific/Engineering Computing, Academy of Mathematics and System Sciences, Chinese Academy of Sciences, P.O. Box 2719, Beijing, 100190, China

1 Introduction

This paper develops and analyzes the following time-harmonic Maxwell equation with the standard impedance boundary condition:

$$\mathbf{curl}\,\mathbf{curl}\,\boldsymbol{E} - \kappa^2 \boldsymbol{E} = \boldsymbol{f} \qquad \text{in } \Omega, \tag{1}$$

$$\mathbf{curl}\,\boldsymbol{E} \times \boldsymbol{\nu} - \mathbf{i}\kappa\lambda \boldsymbol{E}_T = \boldsymbol{g} \qquad \text{on } \partial\Omega, \tag{2}$$

where $\Omega \subset \mathbb{R}^3$ is a bounded C^2-domain and star-shaped with respect to $B_\gamma(x_0)$, $\mathbf{i} = \sqrt{-1}$ denotes the imaginary unit while $\boldsymbol{\nu}$ denotes the unit outward normal to $\partial\Omega$, and $\boldsymbol{E}_T := (\boldsymbol{\nu} \times \boldsymbol{E}) \times \boldsymbol{\nu}$ is the *tangential component* of the electric field $\boldsymbol{E}$. $\kappa > 0$ is called wave number and $\lambda > 0$ is known as the impedance constant. The right hand side $\boldsymbol{f}$ is the current density which is divergence free, i.e., $\mathbf{div}\,\boldsymbol{f} = 0$. The boundary condition is the standard impedance boundary condition which requires $\boldsymbol{g} \cdot \boldsymbol{\nu} = 0$, thus, $\boldsymbol{g}_T = \boldsymbol{g}$. The above time-harmonic Maxwell equation is of considerable importance in the engineering and scientific computation. Throughout this paper, we use notations $A \lesssim B$ and $A \gtrsim B$ for the inequalities $A \leq CB$ and $A \geq CB$, where C is a positive number independent of the mesh size and wave number κ, but the value of which can take on different values in different occurrences. $A \simeq B$ is a shorthand notation for the statement $A \leq CB$ and $B \leq CA$. For simplicity, we suppose $\lambda \simeq 1$, $\kappa > 1$.

The large wave number κ implies the strong indefiniteness of the problem (1)–(2), which brings difficulties both in theoretical analysis and numerical simulation. In [10], the convergence rate of a Trefftz-discontinuous Galerkin approximation method for the homogeneous time-harmonic Maxwell equations with impedance boundary conditions has been derived. Trefftz type methods are non-polynomial finite element methods which are based on special approximation spaces. Functions in these approximation spaces are the local solutions of the considered PDEs. For the time-harmonic Maxwell equation with Dirichlet boundary condition, various finite element methods were developed. In [15, 19], the authors analyzed the error estimates for the Nédélec edge elements. Meanwhile, the interior penalty discontinuous Galerkin (IPDG) method for the time-harmonic equation was introduced and analyzed in [11]. Moreover, stabilized mixed discontinuous Galerkin methods proposed in [12, 17] are based on a mixed formulation of the boundary value problem, which is chosen to provide control on the divergence of the electric field. Furthermore, Brenner, Li, and Sung introduced a locally divergence-free method for the two-dimensional time-harmonic Maxwell equation in [3], where they used the locally divergence-free Crouzeix-Raviart nonconforming P_1 vector fields and included a consistency term involving the jumps of the vector fields across element boundaries. It can also be extended to general three-dimensional domains, but the construction of the locally divergence basis is more complicated (cf. Section 9.3 of [5]). Recently, Feng and Wu [7] proposed and analyzed an interior penalty discontinuous Galerkin (IPDG) method for the problem (1)–(2), which is uniquely solvable without any mesh constraint. Although the DG methods exhibit several advantages over the standard finite element methods, such as flexibilities in constructing trial and test spaces, one obvious disadvantage is that the dimension of the approximation DG space is much larger than the dimension of the corresponding conforming space. For the *hp* finite element discretizations of time-harmonic Maxwell equation, the wavenumber explicit analysis are performed in [14, 16].

Our objective in this paper is to propose a continuous interior penalty finite element method (CIP-FEM) for the time-harmonic Maxwell equation (1)–(2). We use the lowest order space of the second family of Nédélec edge element as the approximation space, but modify the sesquilinear of the classic finite element method by adding a penalty term on the jumps of the tangential component of its vorticity field, i.e.,

$$J(\boldsymbol{E}_h, \boldsymbol{F}_h) := -\mathbf{i} \sum_{\mathcal{F}\in\mathcal{E}_h^I} \gamma_{\mathcal{F}} h_{\mathcal{F}} \langle [\![\mathbf{curl}\, \boldsymbol{E}_h \times \boldsymbol{\nu}_F]\!], [\![\mathbf{curl}\, \boldsymbol{F}_h \times \boldsymbol{\nu}_F]\!]\rangle_{\mathcal{F}},$$

where $\gamma_{\mathcal{F}} \simeq \gamma$ for a positive constant γ and $\gamma > 0$ is an adjustable parameter. Note that if the parameter $\gamma_{\mathcal{F}}$ is replaced by a complex number with positive real part and negative imaginary part, the ideas of the paper can still be applied. Here we set its real part to be zero in the theoretical analysis for the ease of presentation. For the Helmholtz equation, it has been proved in [18] that CIP-FEM performs much better than the standard finite element method, the idea of which was originally proposed by Douglas and Dupont [6] for the second-order elliptic and parabolic problems. However, comparing with the CIP-FEM for the Helmholtz problem, the kernel space of the operator **curl** is not empty which means that the analysis of the CIP-FEM for the time-harmonic Maxwell equation is more tricky than that for the Helmholtz equation. We find that the CIP-FEM for the time-harmonic Maxwell equation attains a unique solution for any $\kappa > 0$, $h > 0$. Let $\boldsymbol{E}_h$ be the CIP-FEM solution of the problem (1)–(2). We can derive that the following stability estimate holds for any quasi-uniform meshes:

$$\kappa^2\|\boldsymbol{E}_h\|_{0,\Omega}^2 + \|\mathbf{curl}\, \boldsymbol{E}_h\|_{0,\Omega}^2 \lesssim C_{\text{stab}}^2\|\boldsymbol{f}\|_{0,\Omega}^2 + \tfrac{C_{\text{stab}}}{\lambda}\|\boldsymbol{g}\|_{0,\partial\Omega}^2 \tag{3}$$

where $C_{\text{stab}} := \frac{1}{\kappa} + \frac{1}{\kappa^2 h\lambda} + \frac{1}{\kappa^3 h^2\gamma}$. Moreover, we have the following error estimates:

$$|||\, \boldsymbol{E} - \boldsymbol{E}_h|||_h \lesssim C_{\kappa h}(1+\gamma)\left(\kappa h + C_{\text{stab}}\kappa^3 h^2\right) M(\boldsymbol{f}, \boldsymbol{g}) \tag{4}$$

where $M(\boldsymbol{f}, \boldsymbol{g}) := \|\boldsymbol{f}\|_{0,\Omega} + \kappa^{-2}\|\mathbf{curl}\, \boldsymbol{f}\|_{0,\Omega} + \kappa^{-2}\|\boldsymbol{f}\times\boldsymbol{\nu}\|_{1/2,\partial\Omega} + \|\boldsymbol{g}\|_{0,\partial\Omega} + \kappa^{-1}\|\boldsymbol{g}\|_{1/2,\partial\Omega}$, $C_{\kappa h}$ denote a generic constant depending on κh which will be defined in Section 4 and the energy norm $|||\cdot|||_h$ is defined as

$$|||\, \boldsymbol{v}|||_h := \left(\|\boldsymbol{v}\|_{\mathbf{curl},h}^2 + \kappa^2\|\boldsymbol{v}\|_{0,\Omega}^2 + \kappa\lambda\|\boldsymbol{v}_T\|_{0,\partial\Omega}^2\right)^{\frac{1}{2}}, \tag{5}$$

where the definition of $\|\cdot\|_{\mathbf{curl},h}$ can be found in (8). We would like to mention that the corresponding error estimate (5.23) in [7] is shown as

$$\|\boldsymbol{E} - \boldsymbol{E}_h\|_{\text{DG}} \lesssim \kappa h + \hat{C}_{\text{sta}}(1+\gamma_1)(\kappa^3 h^2 + \kappa^2 h^{\frac{3}{2}})M(\boldsymbol{f}, \boldsymbol{g}), \tag{6}$$

where the norm of $\|\cdot\|_{\mathrm{DG}}$ is defined as follows

$$\|\boldsymbol{v}\|_{\mathrm{DG}}^2 = \sum_{K\in\mathcal{T}_h} \|\mathbf{curl}\ \boldsymbol{v}\|_{0,K}^2 + \|\boldsymbol{v}\|_{0,\Omega}^2 + \sum_{\mathcal{F}\in\mathcal{E}_h^I} \left(\frac{\gamma_{0,\mathcal{F}}}{h_{\mathcal{F}}} \|[\![\boldsymbol{v}_T]\!]\|_{0,\mathcal{F}}^2 + \gamma_{1,\mathcal{F}} h_{\mathcal{F}} \|[\![\mathbf{curl}\ \boldsymbol{v} \times \boldsymbol{\nu}_F]\!]\|_{0,\mathcal{F}}^2 \right), \tag{7}$$

$\gamma_{0,\mathcal{F}}$ and $\gamma_{1,\mathcal{F}}$ are the penalty parameters to the terms on the jumps of the tangential component of its electric and vorticity field, respectively. $\gamma_1 = \min_{\mathcal{F}\in\mathcal{E}_h^I}\{\gamma_{1,\mathcal{F}}\}$ and we refer to (5.22) in [7] the definition of $\hat{C}_{\mathrm{sta}}$. Comparing with the estimate (5.23) in [7], the lost of half order of h in the theoretical analysis is remedied in our paper.

In practice, the "rule of thumb" is to use 8–10 grid points per wave length, which means that the mesh size h must satisfy the constraint $\kappa h \lesssim 1$. The estimate (4) indicates that the error is not completely controlled by the product κh and it provides evidences of the existence of so-called pollution effect, which can also be observed in the numerical experiments. Moreover, we may obtain the following improved error estimates in the regime $\kappa^3 h^2 \lesssim 1$:

$$|||\boldsymbol{E} - \boldsymbol{E}_h|||_h \lesssim (\kappa h + \kappa^3 h^2) M(\boldsymbol{f}, \boldsymbol{g}).$$

The remainder of this paper is organized as follows: In Section 2, we precisely define the CIP-FEM for the time-harmonic Maxwell equation and give some notations in the next section. Section 3 is devoted to the stability estimates for our CIP-FEM scheme. In Section 4, the stability and regularity results for the Maxwell equations (1)–(2) are given and the error estimates of the CIP-FEM for the time-harmonic Maxwell equation are derived for any $\kappa > 0$, $h > 0$, and $\gamma > 0$. The improved results under the mesh condition that $\kappa^3 h^2$ is small enough are also included. Finally, in Section 5, numerical experiments are demonstrated to confirm our theoretical analysis.

2 Continuous interior penalty finite element method

To formulate the CIP-FEM for the time-harmonic Maxwell equation, we first introduce some notations. We consider a subdivision of Ω into a mesh consisting of shape regular tetrahedra in $\mathbb{R}^3$, and denote the collection of tetrahedra by $\mathcal{T}_h$. In this paper, we investigate quasi-uniform meshes. Let h_K be the diameter of tetrahedron K and $h := \max_{K\in\mathcal{T}_h} h_K$. The collection of faces is denoted by $\mathcal{E}_h$, while the collection of interior faces by $\mathcal{E}_h^I$ and the collection of boundary faces by $\mathcal{E}_h^B$. We also define the jump $[\![\boldsymbol{v}]\!]$ of $\boldsymbol{v}$ on an interior face $\mathcal{F} = \partial K^+ \cap \partial K^-$ as

$$[\![\boldsymbol{v}]\!]|_{\mathcal{F}} := \begin{cases} \boldsymbol{v}|_{K^+} - \boldsymbol{v}|_{K^-} & \text{if the global label of } K^+ \text{ is bigger,} \\ \boldsymbol{v}|_{K^-} - \boldsymbol{v}|_{K^+} & \text{if the global label of } K^- \text{ is bigger.} \end{cases}$$

For every $\mathcal{F} = \partial K^+ \cap \partial K^- \in \mathcal{E}_h^I$, let $\boldsymbol{\nu}_{\mathcal{F}}$ be the unit outward normal to the face $\mathcal{F}$ of the element K^+ if the global label of K^+ is bigger and of the element K^- if the other way around. Throughout this paper, we use the standard notations and definitions for Sobolev spaces (see, e.g., Adams [1]). In particular, $(\cdot,\cdot)_Q$ and $\langle\cdot,\cdot\rangle_\Sigma$ for $Q \subset \Omega$ and $\Sigma \subset \partial\Omega$ denote the L^2-inner product on *complex-valued* $L^2(Q)$ and $L^2(\Sigma)$ spaces, respectively. For a given function space W, let $\boldsymbol{W} = (W)^3$. In particular, $\boldsymbol{L}^2(\Omega) = (L^2(\Omega))^3$ and $\boldsymbol{H}^s(\Omega) = (H^s(\Omega))^3$. Denote by $\|\cdot\|_{s,\Omega}$ the norm on $\boldsymbol{H}^s(\Omega)$ or $H^s(\Omega)$. Let $H(\mathbf{curl},\Omega) := \{\boldsymbol{u} \in \boldsymbol{L}^2(\Omega), \mathbf{curl}\,\boldsymbol{u} \in \boldsymbol{L}^2(\Omega)\}$, the norm of which is defined as follows:

$$\|\boldsymbol{v}\|_{H(\mathbf{curl},\Omega)} := \left(\|\boldsymbol{v}\|_{0,\Omega}^2 + \|\mathbf{curl}\ \boldsymbol{v}\|_{0,\Omega}^2\right)^{\frac{1}{2}} \quad \forall \boldsymbol{v} \in H(\mathbf{curl},\Omega).$$

In the following, we define the "energy" space $\boldsymbol{V}$ as

$$\boldsymbol{V} := H(\mathbf{curl},\Omega) \cap \Pi_{K\in\mathcal{T}_h}\boldsymbol{H}^2(K).$$

The semi-norm of the space $\boldsymbol{V}$ on $\mathcal{T}_h$ are defined as follows:

$$\|\boldsymbol{v}\|_{\mathbf{curl},h} := \left(\sum_{K\in\mathcal{T}_h} \|\mathbf{curl}\ \boldsymbol{v}\|_{0,K}^2 + \sum_{\mathcal{F}\in\mathcal{E}_h^I} \gamma_{\mathcal{F}} h_{\mathcal{F}} \|[\![\mathbf{curl}\ \boldsymbol{v} \times \boldsymbol{\nu}_F]\!]\|_{0,\mathcal{F}}^2\right)^{\frac{1}{2}}, \tag{8}$$

where $\gamma_{\mathcal{F}} \simeq \gamma$ for a positive constant γ. Let $\boldsymbol{V}_h$ be the approximation space which is defined as

$$\boldsymbol{V}_h := \{\boldsymbol{v}_h \in H(\mathbf{curl};\Omega)\ :\ \boldsymbol{v}_h|_K \in (\mathcal{P}_1(K))^3,\ \forall K \in \mathcal{T}_h\},$$

where $\mathcal{P}_1(K)$ denotes the set of linear polynomials on K; in fact, $\boldsymbol{V}_h$ is the lowest order space of the second type of Nédélec edge element. Then our CIP-FEM for the problem (1)–(2) is to find $\boldsymbol{E}_h \in \boldsymbol{V}_h$ such that

$$a_h(\boldsymbol{E}_h, \boldsymbol{F}_h) = (\boldsymbol{f}, \boldsymbol{F}_h) + \langle \boldsymbol{g}, (\boldsymbol{F}_h)_T\rangle_{\partial\Omega} \quad \forall \boldsymbol{F}_h \in \boldsymbol{V}_h, \tag{9}$$

where

$$a_h(\boldsymbol{E}_h, \boldsymbol{F}_h) := b_h(\boldsymbol{E}_h, \boldsymbol{F}_h) - \kappa^2(\boldsymbol{E}_h, \boldsymbol{F}_h) - \mathbf{i}\kappa\lambda\langle(\boldsymbol{E}_h)_T, (\boldsymbol{F}_h)_T\rangle_{\partial\Omega} \tag{10}$$

and

$$b_h(\boldsymbol{E}_h, \boldsymbol{F}_h) := (\mathbf{curl}\ \boldsymbol{E}_h, \mathbf{curl}\ \boldsymbol{F}_h) + J(\boldsymbol{E}_h, \boldsymbol{F}_h). \tag{11}$$

It is clear that this is a consistent discretization formulation which means that if $\boldsymbol{E} \in \boldsymbol{H}^2(\Omega)$, then

$$a_h(\boldsymbol{E} - \boldsymbol{E}_h, \boldsymbol{F}_h) = 0 \quad \forall \boldsymbol{F}_h \in \boldsymbol{V}_h. \tag{12}$$

3 Stability estimates for CIP-FEM

We first derive the stability estimates for our CIP-FEM. Note that $\boldsymbol{E}_h$ is piecewise linear on $\mathcal{T}_h$ and hence $\mathbf{curl}\ \mathbf{curl}\ \boldsymbol{E}_h = 0$ on each element $K \in \mathcal{T}_h$. We first bound $\|\mathbf{curl}\ \boldsymbol{E}_h\|_{0,\Omega}$ by using integration by parts on each element.

Lemma 3.1 *For any* $0 < \epsilon < 1$, *there exists a constant* c_ϵ *which depends only on* ϵ *such that*

$$\|\mathbf{curl}\ \boldsymbol{E}_h\|_{0,\Omega}^2 \leq \epsilon\kappa^2\|\boldsymbol{E}_h\|_{0,\Omega}^2 + \frac{c_\epsilon}{h}\|(\boldsymbol{E}_h)_T\|_{0,\partial\Omega}^2 + \frac{c_\epsilon}{\kappa^2 h^2 \gamma}\sum_{\mathcal{F}\in\mathcal{E}_h^I}\gamma_{\mathcal{F}} h_{\mathcal{F}}\|[\![\mathbf{curl}\ \boldsymbol{E}_h \times \boldsymbol{\nu}_F]\!]\|_{0,\mathcal{F}}^2.$$

Proof Note that $\mathbf{curl}\ \mathbf{curl}\ \boldsymbol{E}_h = 0$ on each element $K \in \mathcal{T}_h$. By the Green's formula we have

$$\begin{aligned}\|\mathbf{curl}\ \boldsymbol{E}_h\|_{0,\Omega}^2 &= \sum_{K\in\mathcal{T}_h}\int_{\partial K}(\mathbf{curl}\ \boldsymbol{E}_h \times \boldsymbol{\nu})(\boldsymbol{E}_h)_T \\ &= \sum_{\mathcal{F}\in\mathcal{E}_h}\int_{\mathcal{F}}[\![\mathbf{curl}\ \boldsymbol{E}_h \times \boldsymbol{\nu}_F]\!](\boldsymbol{E}_h)_T \\ &\leq \sum_{\mathcal{F}\in\mathcal{E}_h^B}\|\mathbf{curl}\ \boldsymbol{E}_h\|_{0,\mathcal{F}}\|(\boldsymbol{E}_h)_T\|_{0,\mathcal{F}} + \sum_{\mathcal{F}\in\mathcal{E}_h^I}\|[\![\mathbf{curl}\ \boldsymbol{E}_h \times \boldsymbol{\nu}_F]\!]\|_{0,\mathcal{F}}\|(\boldsymbol{E}_h)_T\|_{0,\mathcal{F}}.\end{aligned}$$

From the trace inequality, the inverse inequality, and Young's inequality, we may get

$$\begin{aligned}&\|\mathbf{curl}\ \boldsymbol{E}_h\|_{0,\Omega}^2 \leq \epsilon\|\mathbf{curl}\ \boldsymbol{E}_h\|_{0,\Omega}^2 + \frac{C}{\epsilon h}\|(\boldsymbol{E}_h)_T\|_{0,\partial\Omega}^2 \\ &+\epsilon(1-\epsilon)\kappa^2\|\boldsymbol{E}_h\|_{0,\Omega}^2 + \frac{C}{\epsilon(1-\epsilon)\kappa^2 h^2\gamma}\sum_{\mathcal{F}\in\mathcal{E}_h^I}\gamma_{\mathcal{F}} h_{\mathcal{F}}\|[\![\mathbf{curl}\ \boldsymbol{E}_h \times \boldsymbol{\nu}_F]\!]\|_{0,\mathcal{F}}^2,\end{aligned}$$

which implies that Lemma 3.1 holds. □

Then we may derive some reverse inequalities by taking $\boldsymbol{F}_h = \boldsymbol{E}_h$ in (9). Actually, we have

Lemma 3.2 *Let* $\boldsymbol{E}_h$ *be the solution of* (9), *then there hold*

$$\kappa^2\|\boldsymbol{E}_h\|_{0,\Omega}^2 \leq 2\|\mathbf{curl}\ \boldsymbol{E}_h\|_{0,\Omega}^2 + \frac{C}{\kappa^2}\|\boldsymbol{f}\|_{0,\Omega}^2 + \frac{C}{\kappa\lambda}\|\boldsymbol{g}\|_{0,\partial\Omega}^2, \tag{13}$$

$$\begin{aligned}&\sum_{\mathcal{F}\in\mathcal{E}_h^I}\gamma_{\mathcal{F}} h_{\mathcal{F}}\|[\![\mathbf{curl}\ \boldsymbol{E}_h \times \boldsymbol{\nu}_F]\!]\|_{0,\mathcal{F}}^2 + \kappa\lambda\|(\boldsymbol{E}_h)_T\|_{0,\partial\Omega}^2 \\ &\leq \frac{C}{\kappa}\|\boldsymbol{f}\|_{0,\Omega}\|\mathbf{curl}\ \boldsymbol{E}_h\|_{0,\Omega} + \frac{C}{\kappa^2}\|\boldsymbol{f}\|_{0,\Omega}^2 + \frac{C}{\kappa\lambda}\|\boldsymbol{g}\|_{0,\partial\Omega}^2.\end{aligned} \tag{14}$$

Proof Taking $\boldsymbol{F}_h = \boldsymbol{E}_h$ in (9) yields

$$b_h(\boldsymbol{E}_h, \boldsymbol{E}_h) - \kappa^2(\boldsymbol{E}_h, \boldsymbol{E}_h) - \mathbf{i}\kappa\lambda\langle(\boldsymbol{E}_h)_T, (\boldsymbol{E}_h)_T\rangle_{\partial\Omega} = (\boldsymbol{f}, \boldsymbol{E}_h) + \langle\boldsymbol{g}, (\boldsymbol{E}_h)_T\rangle_{\partial\Omega}.$$

Therefore, by taking real part and imaginary part of the above equation, we get

$$\kappa^2\|\boldsymbol{E}_h\|_{0,\Omega}^2 - \|\mathbf{curl}\,\boldsymbol{E}_h\|_{0,\Omega}^2 \le |(\boldsymbol{f},\boldsymbol{E}_h) + \langle \boldsymbol{g}, (\boldsymbol{E}_h)_T\rangle_{\partial\Omega}|, \tag{15}$$

$$\sum_{\mathcal{F}\in\mathcal{E}_h^I} \gamma_{\mathcal{F}} h_{\mathcal{F}} \|[\![\mathbf{curl}\,\boldsymbol{E}_h \times \boldsymbol{\nu}_F]\!]\|_{0,\mathcal{F}}^2 + \kappa\lambda\|(\boldsymbol{E}_h)_T\|_{0,\partial\Omega}^2 \le |(\boldsymbol{f},\boldsymbol{E}_h) + \langle \boldsymbol{g}, (\boldsymbol{E}_h)_T\rangle_{\partial\Omega}|. \tag{16}$$

By (16) and Young's inequality , we obtain

$$\begin{aligned}
&\sum_{\mathcal{F}\in\mathcal{E}_h^I} \gamma_{\mathcal{F}} h_{\mathcal{F}} \|[\![\mathbf{curl}\,\boldsymbol{E}_h \times \boldsymbol{\nu}_F]\!]\|_{0,\mathcal{F}}^2 + \kappa\lambda\|(\boldsymbol{E}_h)_T\|_{0,\partial\Omega}^2\\
&\le \|\boldsymbol{f}\|_{0,\Omega}\|\boldsymbol{E}_h\|_{0,\Omega} + \frac{1}{2\kappa\lambda}\|\boldsymbol{g}\|_{0,\partial\Omega}^2 + \frac{\kappa\lambda}{2}\|(\boldsymbol{E}_h)_T\|_{0,\partial\Omega}^2,
\end{aligned}$$

which implies

$$\begin{aligned}
&\sum_{\mathcal{F}\in\mathcal{E}_h^I} \gamma_{\mathcal{F}} h_{\mathcal{F}} \|[\![\mathbf{curl}\,\boldsymbol{E}_h \times \boldsymbol{\nu}_F]\!]\|_{0,\mathcal{F}}^2 + \frac{\kappa\lambda}{2}\|(\boldsymbol{E}_h)_T\|_{0,\partial\Omega}^2\\
&\le \|\boldsymbol{f}\|_{0,\Omega}\|\boldsymbol{E}_h\|_{0,\Omega} + \frac{1}{2\kappa\lambda}\|\boldsymbol{g}\|_{0,\partial\Omega}^2.
\end{aligned} \tag{17}$$

On the other hand, by (15) and Young's inequality, we have

$$\kappa^2\|\boldsymbol{E}_h\|_{0,\Omega}^2 \le \|\mathbf{curl}\,\boldsymbol{E}_h\|_{0,\Omega}^2 + \|\boldsymbol{f}\|_{0,\Omega}\|\boldsymbol{E}_h\|_{0,\Omega} + \frac{1}{2\kappa\lambda}\|\boldsymbol{g}\|_{0,\partial\Omega}^2 + \frac{\kappa\lambda}{2}\|(\boldsymbol{E}_h)_T\|_{0,\partial\Omega}^2.$$

Combining the above estimate with (17) and using Young's inequality yields

$$\begin{aligned}
\kappa^2\|\boldsymbol{E}_h\|_{0,\Omega}^2 &\le \|\mathbf{curl}\,\boldsymbol{E}_h\|_{0,\Omega}^2 + 2\|\boldsymbol{f}\|_{0,\Omega}\|\boldsymbol{E}_h\|_{0,\Omega} + \frac{1}{\kappa\lambda}\|\boldsymbol{g}\|_{0,\partial\Omega}^2\\
&\le \|\mathbf{curl}\,\boldsymbol{E}_h\|_{0,\Omega}^2 + \frac{2}{\kappa^2}\|\boldsymbol{f}\|_{0,\Omega}^2 + \frac{\kappa^2}{2}\|\boldsymbol{E}_h\|_{0,\Omega}^2 + \frac{1}{\kappa\lambda}\|\boldsymbol{g}\|_{0,\partial\Omega}^2,
\end{aligned}$$

which indicates that (13) holds. Plugging (13) into the right-hand side of (17) and utilizing Young's inequality, we get

$$\begin{aligned}
&\sum_{\mathcal{F}\in\mathcal{E}_h^I} \gamma_{\mathcal{F}} h_{\mathcal{F}} \|[\![\mathbf{curl}\,\boldsymbol{E}_h \times \boldsymbol{\nu}_F]\!]\|_{0,\mathcal{F}}^2 + \frac{\kappa\lambda}{2}\|(\boldsymbol{E}_h)_T\|_{0,\partial\Omega}^2\\
&\le \frac{C}{\kappa}\|\boldsymbol{f}\|_{0,\Omega}\left(\|\mathbf{curl}\,\boldsymbol{E}_h\|_{0,\Omega} + \frac{1}{\kappa}\|\boldsymbol{f}\|_{0,\Omega} + \frac{1}{(\kappa\lambda)^{\frac{1}{2}}}\|\boldsymbol{g}\|_{0,\partial\Omega}\right) + \frac{1}{2\kappa\lambda}\|\boldsymbol{g}\|_{0,\partial\Omega}^2\\
&\le \frac{C}{\kappa}\|\boldsymbol{f}\|_{0,\Omega}\|\mathbf{curl}\,\boldsymbol{E}_h\|_{0,\Omega} + \frac{C}{\kappa^2}\|\boldsymbol{f}\|_{0,\Omega}^2 + \frac{C}{\kappa\lambda}\|\boldsymbol{g}\|_{0,\partial\Omega}^2,
\end{aligned}$$

which completes the proof of the lemma. □

Remark 1 If $\gamma_{\mathcal{F}}$ is replaced by a complex number with positive real part and negative imaginary part, (15) and (16) still hold, which indicate that Lemma 3.2 is still true under this situation. In fact, the theoretical analysis for CIP-FEM can be extended to the case when $\gamma_{\mathcal{F}}$ is a complex number with positive real part and negative imaginary part.

Combining Lemma 3.1 and Lemma 3.2 together, we may further derive the following stability estimates for our CIP-FEM.

Theorem 3.1 *Let $\boldsymbol{E}_h$ be the solution of (9), then there hold the following stability estimates:*

$$\kappa^2\|\boldsymbol{E}_h\|_{0,\Omega}^2 + \|\mathbf{curl}\ \boldsymbol{E}_h\|_{0,\Omega}^2 \lesssim C_{\rm stab}^2\|\boldsymbol{f}\|_{0,\Omega}^2 + \frac{C_{\rm stab}}{\lambda}\|\boldsymbol{g}\|_{0,\partial\Omega}^2, \tag{18}$$

and

$$\sum_{\mathcal{F}\in\mathcal{E}_h^I}\gamma_{\mathcal{F}}h_{\mathcal{F}}\|[\![\mathbf{curl}\ \boldsymbol{E}_h\times\boldsymbol{\nu}_F]\!]\|_{0,\mathcal{F}}^2 + \kappa\lambda\|(\boldsymbol{E}_h)_T\|_{0,\partial\Omega}^2 \lesssim \frac{C_{\rm stab}}{\kappa}\|\boldsymbol{f}\|_{0,\Omega}^2 + \frac{1}{\kappa\lambda}\|\boldsymbol{g}\|_{0,\partial\Omega}^2, \tag{19}$$

here

$$C_{\rm stab} := \frac{1}{\kappa} + \frac{1}{\kappa^2 h\lambda} + \frac{1}{\kappa^3 h^2\gamma}.$$

Proof By taking $\epsilon = \frac{1}{3}$ in Lemma 3.1, applying Lemma 3.2, and using Young's inequality, we have

$$\begin{aligned}
&\|\mathbf{curl}\ \boldsymbol{E}_h\|_{0,\Omega}^2 \le \frac{1}{3}\kappa^2\|\boldsymbol{E}_h\|_{0,\Omega}^2 + \frac{C}{h}\|(\boldsymbol{E}_h)_T\|_{0,\partial\Omega}^2 \\
&+\frac{C}{\kappa^2h^2\gamma}\sum_{\mathcal{F}\in\mathcal{E}_h^I}\gamma_{\mathcal{F}}h_{\mathcal{F}}\|[\![\mathbf{curl}\ \boldsymbol{E}_h\times\boldsymbol{\nu}_F]\!]\|_{0,\mathcal{F}}^2 \\
&\le \frac{1}{3}\left(2\|\mathbf{curl}\ \boldsymbol{E}_h\|_{0,\Omega}^2 + \frac{C}{\kappa^2}\|\boldsymbol{f}\|_{0,\Omega}^2 + \frac{C}{\kappa\lambda}\|\boldsymbol{g}\|_{0,\partial\Omega}^2\right) \\
&\quad +C\left(\frac{1}{\kappa h\lambda} + \frac{1}{\kappa^2h^2\gamma}\right)\left(\frac{1}{\kappa}\|\boldsymbol{f}\|_{0,\Omega}\|\mathbf{curl}\ \boldsymbol{E}_h\|_{0,\Omega} + \frac{1}{\kappa^2}\|\boldsymbol{f}\|_{0,\Omega}^2 + \frac{1}{\kappa\lambda}\|\boldsymbol{g}\|_{0,\partial\Omega}^2\right) \\
&\le \frac{2}{3}\|\mathbf{curl}\ \boldsymbol{E}_h\|_{0,\Omega}^2 + \frac{C}{\kappa}\left(\frac{1}{\kappa h\lambda} + \frac{1}{\kappa^2h^2\gamma}\right)\|\boldsymbol{f}\|_{0,\Omega}\|\mathbf{curl}\ \boldsymbol{E}_h\|_{0,\Omega} \\
&\quad +C\left(1 + \frac{1}{\kappa h\lambda} + \frac{1}{\kappa^2h^2\gamma}\right)\left(\frac{1}{\kappa^2}\|\boldsymbol{f}\|_{0,\Omega}^2 + \frac{1}{\kappa\lambda}\|\boldsymbol{g}\|_{0,\partial\Omega}^2\right) \\
&\le \frac{5}{6}\|\mathbf{curl}\ \boldsymbol{E}_h\|_{0,\Omega}^2 + C\left(1 + \frac{1}{\kappa h\lambda} + \frac{1}{\kappa^2h^2\gamma}\right)^2\frac{1}{\kappa^2}\|\boldsymbol{f}\|_{0,\Omega}^2 \\
&\quad +C\left(1 + \frac{1}{\kappa h\lambda} + \frac{1}{\kappa^2h^2\gamma}\right)\frac{1}{\kappa\lambda}\|\boldsymbol{g}\|_{0,\partial\Omega}^2.
\end{aligned}$$

Hence,

$$\|\mathbf{curl}\, \boldsymbol{E}_h\|_{0,\Omega}^2 \lesssim C_{\text{stab}}^2 \|\boldsymbol{f}\|_{0,\Omega}^2 + \frac{C_{\text{stab}}}{\lambda} \|\boldsymbol{g}\|_{0,\partial\Omega}^2,$$

which, together with Lemma 3.2, concludes the proof of this theorem. □

4 Error estimates

In this section, we first recall the regularity estimates for the Maxwell equations (1)–(2) with explicit dependence on the wave number κ. Then we introduce an elliptic projection of the solution $\boldsymbol{E}$ of the problem (1)–(2), and give some estimates for the projection. Furthermore, by exploiting the stability estimates derived in the above section, we may get the error estimates for our CIP-FEM. In what follows, for brevity we denote $C_{\kappa h}$ a generic constant depending on κh, the value of which belongs to the set $\{1 + \sqrt{\kappa h}, 1 + \kappa h + \kappa^2 h^2\}$.

4.1 Stability and regularity estimates

We first recall the following H^1 and L^2 estimates from [9] and [7].

Theorem 4.1 *Let $\boldsymbol{E}$ be the solution of the problem (1)–(2) and $\Omega \subset \mathbb{R}^3$ be a bounded C^2-domain and star-shaped with respect to $B_\gamma(x_0)$. Then*

$$\begin{aligned} &\|\mathbf{curl}\, \boldsymbol{E}\|_{1,\Omega} + \kappa \, \|\mathbf{curl}\, \boldsymbol{E}\|_{0,\Omega} + \kappa \, \|\boldsymbol{E}\|_{1,\Omega} + \kappa^2 \, \|\boldsymbol{E}\|_{0,\Omega} \\ &\lesssim \kappa(\|\boldsymbol{f}\|_{0,\Omega} + \|\boldsymbol{g}\|_{0,\partial\Omega}) + \|\boldsymbol{g}\|_{\frac{1}{2},\partial\Omega}, \end{aligned}$$

where

$$\|\boldsymbol{g}\|_{\frac{1}{2},\partial\Omega} = \inf_{\substack{\boldsymbol{v}\in \boldsymbol{H}^1(\Omega) \\ \boldsymbol{v}=g \text{ on } \partial\Omega}} \|\boldsymbol{v}\|_{1,\Omega}. \tag{20}$$

The following theorem gives H^2 estimates with explicit dependence on κ for (1)–(2), which plays an important role in the error estimates of our CIP-FEM.

Theorem 4.2 *Let $\Omega \subset \mathbb{R}^3$ be a bounded C^2-domain and star-shaped with respect to $B_\gamma(x_0)$. In addition to the assumptions made on $\boldsymbol{f}$, $\boldsymbol{g}$ in Section 1, we assume that $\boldsymbol{f} \in \boldsymbol{H}^1(\Omega)$ and $\boldsymbol{g} \in \boldsymbol{H}^{\frac{1}{2}}(\partial\Omega)$. Then there exists one constant C independent of κ, but depending on Ω and λ, such that*

$$\|\boldsymbol{E}\|_{2,\Omega} \lesssim \kappa M(\boldsymbol{f}, \boldsymbol{g}) \tag{21}$$

where

$$\begin{aligned} M(\boldsymbol{f}, \boldsymbol{g}) := \; &\|\boldsymbol{f}\|_{0,\Omega} + \kappa^{-2} \, \|\mathbf{curl}\, \boldsymbol{f}\|_{0,\Omega} + \kappa^{-2} \, \|\boldsymbol{f} \times \boldsymbol{\nu}\|_{1/2,\partial\Omega} \\ &+ \|\boldsymbol{g}\|_{0,\partial\Omega} + \kappa^{-1} \, \|\boldsymbol{g}\|_{1/2,\partial\Omega} \, . \end{aligned}$$

Proof Taking $m = 2$ in [13, Theorem 3.4] and using Theorem 2.2 in [13] completes the proof of the theorem. □

4.2 $H(\mathbf{curl}, \Omega)$-elliptic projection and its error estimates

Let $\boldsymbol{E}$ be the solution of the problem (1)–(2) and $\widetilde{\boldsymbol{E}}_h \in \boldsymbol{V}_h$ be its $\boldsymbol{H}(\mathbf{curl}, \Omega)$-elliptic projection, which is defined as follows:

$$\widehat{a}_h(\boldsymbol{E} - \widetilde{\boldsymbol{E}}_h, \boldsymbol{F}_h) = 0 \quad \forall \boldsymbol{F}_h \in \boldsymbol{V}_h, \tag{22}$$

where

$$\widehat{a}_h(\boldsymbol{v}, \boldsymbol{w}) := b_h(\boldsymbol{v}, \boldsymbol{w}) + \kappa^2(\boldsymbol{v}, \boldsymbol{w}) - \mathbf{i}\kappa\lambda\langle \boldsymbol{v}_T, \boldsymbol{w}_T\rangle_{\partial\Omega}.$$

The following lemma gives the continuity and coercivity of the sesquilinear form $\widehat{a}_h$. The proof is straightforward, so we omit it.

Lemma 4.1 *For any $\boldsymbol{v}$, $\boldsymbol{w} \in \boldsymbol{V}$, there hold*

$$|\widehat{a}_h(\boldsymbol{v}, \boldsymbol{w})| \le |||\boldsymbol{v}|||_h \, |||\boldsymbol{w}|||_h, \tag{23}$$

$$\operatorname{Re} \widehat{a}_h(\boldsymbol{v}, \boldsymbol{v}) - \operatorname{Im} \widehat{a}_h(\boldsymbol{v}, \boldsymbol{v}) = |||\boldsymbol{v}|||_h^2. \tag{24}$$

Denote π_N as the interpolation onto the second-type Nédélec edge element space $\boldsymbol{V}_h$. The following lemma gives the interpolation error estimates.

Lemma 4.2 *Suppose $\boldsymbol{E} \in \boldsymbol{H}^2(\Omega)$. Then*

$$\|\boldsymbol{E} - \pi_N \boldsymbol{E}\|_{0,\Omega} \lesssim h^2 \|\boldsymbol{E}\|_{2,\Omega}, \tag{25}$$

$$\|(\boldsymbol{E} - \pi_N \boldsymbol{E})_T\|_{0,\partial\Omega} + h^{\frac{1}{2}} \|(\boldsymbol{E} - \pi_N \boldsymbol{E})_T\|_{\frac{1}{2},\partial\Omega} \lesssim h^{\frac{3}{2}} \|\boldsymbol{E}\|_{2,\Omega}, \tag{26}$$

$$\|\boldsymbol{E} - \pi_N \boldsymbol{E}\|_{H(\mathbf{curl},\Omega)} \lesssim h \|\boldsymbol{E}\|_{H^1(\mathbf{curl},\Omega)}, \tag{27}$$

$$|||\boldsymbol{E} - \pi_N \boldsymbol{E}|||_h \lesssim (1+\gamma)^{\frac{1}{2}} h \|\boldsymbol{E}\|_{H^1(\mathbf{curl},\Omega)} + C_{\kappa h} (\kappa h)^{\frac{1}{2}} h \|\boldsymbol{E}\|_{2,\Omega}, \tag{28}$$

where $H^1(\mathbf{curl}, \Omega) := \{\boldsymbol{u} \in \boldsymbol{H}^1(\Omega), \mathbf{curl}\ \boldsymbol{u} \in \boldsymbol{H}^1(\Omega)\}$, the norm of space $H^1(\mathbf{curl}, \Omega)$ is defined as follows:

$$\|\boldsymbol{v}\|_{H^1(\mathbf{curl},\Omega)} := \left(\|\boldsymbol{v}\|_{1,\Omega}^2 + \|\mathbf{curl}\ \boldsymbol{v}\|_{1,\Omega}^2\right)^{\frac{1}{2}} \quad \forall \boldsymbol{v} \in H^1(\mathbf{curl}, \Omega).$$

Proof It follows from [15] that (25)–(27) hold. (28) follows from (25)–(27), the definition (5) of the norm $|||\cdot|||_h$, and the trace inequality. The proof is completed. □

Next, we derive error estimates for $\boldsymbol{E} - \widetilde{\boldsymbol{E}}_h$. Denote by $\widehat{\boldsymbol{E}}_h := \pi_N \boldsymbol{E}$ and $\boldsymbol{\Phi}_h := \widetilde{\boldsymbol{E}}_h - \widehat{\boldsymbol{E}}_h$. The following theorem gives the error estimate in the energy norm.

Theorem 4.3 *Suppose that the solution of problem (1)–(2) is $\boldsymbol{H}^2$ regular, then there hold*

$$|||\boldsymbol{E} - \widetilde{\boldsymbol{E}}_h|||_h \lesssim |||\boldsymbol{E} - \widehat{\boldsymbol{E}}_h|||_h \lesssim (1+\gamma)^{\frac{1}{2}} h \|\boldsymbol{E}\|_{H^1(\mathbf{curl},\Omega)} + C_{\kappa h} (\kappa h)^{\frac{1}{2}} h \|\boldsymbol{E}\|_{2,\Omega}. \tag{29}$$

Proof From (22), we have

$$\widehat{a}_h(\boldsymbol{\Phi}_h, \boldsymbol{\Phi}_h) = \widehat{a}_h(\boldsymbol{E} - \widehat{\boldsymbol{E}}_h, \boldsymbol{\Phi}_h). \tag{30}$$

From Lemma 4.1 and (30), we may get

$$\begin{aligned}|||\boldsymbol{\Phi}_h|||_h^2 &= \operatorname{Re}\widehat{a}_h(\boldsymbol{\Phi}_h, \boldsymbol{\Phi}_h) - \operatorname{Im}\widehat{a}_h(\boldsymbol{\Phi}_h, \boldsymbol{\Phi}_h)\\ &= \operatorname{Re}\widehat{a}_h(\boldsymbol{E} - \widehat{\boldsymbol{E}}_h, \boldsymbol{\Phi}_h) - \operatorname{Im}\widehat{a}_h(\boldsymbol{E} - \widehat{\boldsymbol{E}}_h, \boldsymbol{\Phi}_h)\\ &\lesssim |||\boldsymbol{E} - \widehat{\boldsymbol{E}}_h|||_h\, |||\boldsymbol{\Phi}_h|||_h .\end{aligned}$$

This means that

$$|||\boldsymbol{\Phi}_h|||_h \lesssim |||\boldsymbol{E} - \widehat{\boldsymbol{E}}_h|||_h, \tag{31}$$

which, together with the triangle inequality, yields

$$|||\boldsymbol{E} - \widetilde{\boldsymbol{E}}_h|||_h \lesssim |||\boldsymbol{E} - \widehat{\boldsymbol{E}}_h|||_h .$$

Then the proof of the theorem follows from (28). □

Next we use the duality argument to estimate the L^2 norm of $\boldsymbol{E} - \widetilde{\boldsymbol{E}}_h$. Let $U_h := \{u \in H^1(\Omega) : u|_K \in \mathcal{P}_2(K), \forall K \in \mathcal{T}_h\}$, where $\mathcal{P}_2(K)$ is the set of quadratic polynomials on K. Let $U_h^0 := U_h \cap H_0^1(\Omega)$ and $\boldsymbol{V}_h^0 := \boldsymbol{V}_h \cap H_0(\mathbf{curl}, \Omega)$ where $H_0(\mathbf{curl}, \Omega) := \{\boldsymbol{u} \in H(\mathbf{curl}, \Omega), \boldsymbol{u} \times \boldsymbol{\nu} = 0 \text{ on } \partial\Omega\}$. Obviously ∇U_h and ∇U_h^0 are subspaces of $\boldsymbol{V}_h$ and $\boldsymbol{V}_h^0$, respectively. The following lemma gives both the Helmholtz decomposition and discrete Helmholtz decomposition for each $\boldsymbol{v}_h \in \boldsymbol{V}_h$.

Lemma 4.3

(i) For $\boldsymbol{v}_h \in \boldsymbol{V}_h^0$, there exist $r \in H_0^1(\Omega)$, $r_h \in U_h^0$, $\boldsymbol{w} \in H_0(\mathbf{curl}, \Omega)$, and $\boldsymbol{w}_h \in \boldsymbol{V}_h^0$, such that

$$\boldsymbol{v}_h = \nabla r + \boldsymbol{w} = \nabla r_h + \boldsymbol{w}_h, \tag{32}$$

$$\mathbf{div}\, \boldsymbol{w} = 0 \text{ in } \Omega, \quad (\boldsymbol{w}_h, \nabla\psi_h) = 0 \quad \forall \psi_h \in U_h^0, \tag{33}$$

$$\|\boldsymbol{w} - \boldsymbol{w}_h\|_{0,\Omega} \lesssim h\|\mathbf{curl}\, \boldsymbol{v}_h\|_{0,\Omega}. \tag{34}$$

(ii) For $\boldsymbol{v}_h \in \boldsymbol{V}_h$, there exist $r \in H^1(\Omega)$, $r_h \in U_h$, $\boldsymbol{w} \in H(\mathbf{curl}, \Omega)$, and $\boldsymbol{w}_h \in \boldsymbol{V}_h$, such that

$$\boldsymbol{v}_h = \nabla r + \boldsymbol{w} = \nabla r_h + \boldsymbol{w}_h, \tag{35}$$

$$\mathbf{div}\, \boldsymbol{w} = 0 \text{ in } \Omega, \quad \boldsymbol{w}\cdot\boldsymbol{\nu} = 0 \text{ on } \partial\Omega, \quad (\boldsymbol{w}_h, \nabla\psi_h) = 0 \quad \forall \psi_h \in U_h, \tag{36}$$

$$\|\boldsymbol{w} - \boldsymbol{w}_h\|_{0,\Omega} \lesssim h\|\mathbf{curl}\, \boldsymbol{v}_h\|_{0,\Omega}. \tag{37}$$

Proof For the first part of the lemma, we refer to [15, Theorem 3.45], [15, Lemma 7.6], or [11, Lemma 4.4]. The second part may be proved by using [15, Remark 3.46] and following the proof of [15, Lemma 7.6]. We omit the details. □

In order to remedy the lost half order of h in the error estimates in [7], we need the following Lemmas 4.4-4.7 to establish the building blocks of the proof for Theorem 4.4.

The following lemma converts the estimate $\|\boldsymbol{E} - \widetilde{\boldsymbol{E}}_h\|_{0,\Omega}$ to the estimate of $\|(\boldsymbol{E} - \widetilde{\boldsymbol{E}}_h)_T\|_{0,\partial\Omega}$.

Lemma 4.4 *Let $\widetilde{\boldsymbol{E}}_h$ be the solution to (22), then*

$$\|\boldsymbol{E} - \widetilde{\boldsymbol{E}}_h\|_{0,\Omega} \lesssim h^{\frac{1}{2}}\|(\boldsymbol{E} - \widetilde{\boldsymbol{E}}_h)_T\|_{0,\partial\Omega} + h^{\frac{1}{2}}\|(\boldsymbol{E} - \widehat{\boldsymbol{E}}_h)_T\|_{0,\partial\Omega} + \|\boldsymbol{E} - \widehat{\boldsymbol{E}}_h\|_{0,\Omega} + C_{\kappa h}\,(1+\gamma)^{\frac{1}{2}}\, h\, |||\, \boldsymbol{E} - \widehat{\boldsymbol{E}}_h\, |||_h\,. \tag{38}$$

Proof Recall that we denote by $\boldsymbol{\Phi}_h := \widetilde{\boldsymbol{E}}_h - \widehat{\boldsymbol{E}}_h$ where $\widehat{\boldsymbol{E}}_h := \pi_N \boldsymbol{E}$. According to Proposition 4.5 in [11], there exists $\boldsymbol{\Phi}_h^c \in H_0(\mathbf{curl}, \Omega) \cap \boldsymbol{V}_h$ such that

$$\|\boldsymbol{\Phi}_h - \boldsymbol{\Phi}_h^c\|_{0,\Omega} + h\|\mathbf{curl}\,(\boldsymbol{\Phi}_h - \boldsymbol{\Phi}_h^c)\|_{0,\Omega} \lesssim h^{\frac{1}{2}}\|(\boldsymbol{\Phi}_h)_T\|_{0,\partial\Omega}, \tag{39}$$

From Lemma 4.3(i), we have the following discrete Helmholtz decomposition for $\boldsymbol{\Phi}_h^c$:

$$\boldsymbol{\Phi}_h^c = \boldsymbol{w}_h^0 + \nabla r_h^0, \tag{40}$$

where $r_h^0 \in U_h^0$ and $\boldsymbol{w}_h^0 \in \boldsymbol{V}_h^0$ is discrete divergence free. Moreover, there exists $\boldsymbol{w}^0 \in H_0(\mathbf{curl}, \Omega)$ such that $\mathbf{div}\ \boldsymbol{w}^0 = 0$, $\mathbf{curl}\ \boldsymbol{w}^0 = \mathbf{curl}\ \boldsymbol{\Phi}_h^c$, and

$$\|\boldsymbol{w}_h^0 - \boldsymbol{w}^0\|_{0,\Omega} \lesssim h\|\mathbf{curl}\ \boldsymbol{w}_h^0\|_{0,\Omega} = h\|\mathbf{curl}\ \boldsymbol{\Phi}_h^c\|_{0,\Omega}. \tag{41}$$

From (22), we know that

$$(\boldsymbol{E} - \widetilde{\boldsymbol{E}}_h, \nabla\phi_h^0) = 0 \quad \forall \phi_h^0 \in U_h^0. \tag{42}$$

Next, we introduce the following dual problem:

$$\mathbf{curl}\ \mathbf{curl}\ \boldsymbol{\Psi} + \kappa^2\boldsymbol{\Psi} = \boldsymbol{w}^0 \qquad \text{in } \Omega, \tag{43}$$

$$\mathbf{curl}\ \boldsymbol{\Psi} \times \boldsymbol{\nu} + \mathbf{i}\kappa\lambda\boldsymbol{\Psi}_T = 0 \qquad \text{on } \partial\Omega. \tag{44}$$

It is obvious that $\boldsymbol{\Psi}$ satisfies the following weak formulation:

$$a(\boldsymbol{\Psi}, \boldsymbol{v}) = (\boldsymbol{w}^0, v) \quad \forall \boldsymbol{v} \in H(\mathbf{curl}, \Omega), \tag{45}$$

where

$$a(\boldsymbol{\Psi}, \boldsymbol{v}) := (\mathbf{curl}\ \boldsymbol{\Psi}, \mathbf{curl}\ \boldsymbol{v}) + \kappa^2(\boldsymbol{\Psi}, \boldsymbol{v}) + \mathbf{i}\kappa\lambda\langle\boldsymbol{\Psi}_T, \boldsymbol{v}_T\rangle_{\partial\Omega}.$$

Taking $\boldsymbol{v} = \boldsymbol{\Psi}$ in (45), we can get

$$\|\mathbf{curl}\ \boldsymbol{\Psi}\|_{0,\Omega}^2 + \kappa^2\|\boldsymbol{\Psi}\|_{0,\Omega}^2 + \mathbf{i}\kappa\lambda\,\|\boldsymbol{\Psi}_T\|_{0,\partial\Omega}^2 = (\boldsymbol{w}^0, \boldsymbol{\Psi}),$$

from which we can derive

$$\kappa^2\|\boldsymbol{\Psi}\|_{0,\Omega}^2 \le \left\|\boldsymbol{w}^0\right\|_{0,\Omega}\|\boldsymbol{\Psi}\|_{0,\Omega}\,, \tag{46}$$

and

$$\|\mathbf{curl}\ \boldsymbol{\Psi}\|_{0,\Omega}^2 \le \left\|\boldsymbol{w}^0\right\|_{0,\Omega}\|\boldsymbol{\Psi}\|_{0,\Omega}\,. \tag{47}$$

It is easy to find that (46) implies

$$\|\boldsymbol{\Psi}\|_{0,\Omega} \lesssim \kappa^{-2}\left\|\boldsymbol{w}^0\right\|_{0,\Omega},$$

which combines with (47) yields

$$\|\mathbf{curl}\ \boldsymbol{\Psi}\|_{0,\Omega} \lesssim \kappa^{-1}\left\|\boldsymbol{w}^0\right\|_{0,\Omega}.$$

With the estimate of $\|\boldsymbol{\Psi}\|_{0,\Omega}$ and $\|\mathbf{curl}\ \boldsymbol{\Psi}\|_{0,\Omega}$, following the proof of Theorem 3.2 and Theorem 3.4 and using Theorem 2.2 in [13], we can get

$$\kappa\|\boldsymbol{\Psi}\|_{1,\Omega} + \|\mathbf{curl}\ \boldsymbol{\Psi}\|_{1,\Omega} \lesssim \|\boldsymbol{w}^0\|_{0,\Omega}, \tag{48}$$

and

$$\begin{aligned}\|\boldsymbol{\Psi}\|_{2,\Omega} &\lesssim \|\boldsymbol{w}^0\|_{0,\Omega} + \kappa^{-2}\|\boldsymbol{w}^0\|_{1,\Omega}\\ &\lesssim \|\boldsymbol{w}^0\|_{0,\Omega} + \kappa^{-2}\|\ \mathbf{curl}\ \boldsymbol{w}^0\|_{0,\Omega} = \|\boldsymbol{w}^0\|_{0,\Omega} + \kappa^{-2}\|\mathbf{curl}\ \boldsymbol{\Phi}_h^c\|_{0,\Omega}.\end{aligned} \tag{49}$$

Using (43)–(44), , and Green's formula, we obtain

$$\begin{aligned}&(\boldsymbol{E} - \widetilde{\boldsymbol{E}}_h, \boldsymbol{w}^0) = (\boldsymbol{E} - \widetilde{\boldsymbol{E}}_h, \mathbf{curl\ curl}\ \boldsymbol{\Psi} + \kappa^2\boldsymbol{\Psi})\\ &= (\mathbf{curl}\ (\boldsymbol{E} - \widetilde{\boldsymbol{E}}_h), \mathbf{curl}\ \boldsymbol{\Psi}) - \mathbf{i}\kappa\lambda\langle(\boldsymbol{E} - \widetilde{\boldsymbol{E}}_h)_T, \boldsymbol{\Psi}_T\rangle_{\partial\Omega} + \kappa^2(\boldsymbol{E} - \widetilde{\boldsymbol{E}}_h, \boldsymbol{\Psi})\\ &= \widehat{a}_h(\boldsymbol{E} - \widetilde{\boldsymbol{E}}_h, \boldsymbol{\Psi}) = \widehat{a}_h(\boldsymbol{E} - \widetilde{\boldsymbol{E}}_h, \boldsymbol{\Psi} - \widehat{\boldsymbol{\Psi}}_h),\end{aligned} \tag{50}$$

where $\widehat{\boldsymbol{\Psi}}_h := \pi_N\boldsymbol{\Psi} \in \boldsymbol{V}_h$ is the interpolation approximation of $\boldsymbol{\Psi}$ in $\boldsymbol{V}_h$. From the definition of $b_h(\cdot,\cdot)$ and $|||\cdot|||_h$, we have

$$\begin{aligned}|b_h(\boldsymbol{E} - \widetilde{\boldsymbol{E}}_h, \boldsymbol{\Psi} - \widehat{\boldsymbol{\Psi}}_h)| \lesssim\ &|||\boldsymbol{E} - \widetilde{\boldsymbol{E}}_h\ |||_h \big(\|\ \mathbf{curl}\ (\boldsymbol{\Psi} - \widehat{\boldsymbol{\Psi}}_h)\|_{0,\Omega}\\ &+ \big(\sum_{\mathcal{F}\in\mathcal{E}_h^I} \gamma h_{\mathcal{F}}||[\mathbf{curl}\ (\boldsymbol{\Psi} - \widehat{\boldsymbol{\Psi}}_h) \times \boldsymbol{\nu}_F]||_{0,\mathcal{F}}^2\big)^{\frac{1}{2}}\big).\end{aligned} \tag{51}$$

Obviously the first term in (51) can be bounded by $|||\boldsymbol{E} - \widetilde{\boldsymbol{E}}_h\ |||_h\ h\|\boldsymbol{\Psi}\|_{H^1(\mathbf{curl},\Omega)}$; next, we focus on the estimate of the second term in (51).

Let $T := \sum_{\mathcal{F}\in\mathcal{E}_h^I} \gamma h_{\mathcal{F}}||\mathbf{curl}\ (\boldsymbol{\Psi} - \widehat{\boldsymbol{\Psi}}_h)||_{0,\mathcal{F}}^2$, using the triangle inequality, we get

$$T \lesssim \sum_{\mathcal{F}\in\mathcal{E}_h^I} h_{\mathcal{F}}||\mathbf{curl}\ \boldsymbol{\Psi} - \Pi_h\mathbf{curl}\ \boldsymbol{\Psi}||_{0,\mathcal{F}}^2 + \sum_{\mathcal{F}\in\mathcal{E}_h^I} h_{\mathcal{F}}||\Pi_h\mathbf{curl}\ \boldsymbol{\Psi} - \mathbf{curl}\ \widehat{\boldsymbol{\Psi}}_h)||_{0,\mathcal{F}}^2, \tag{52}$$

where Π_h is the L^2 projection to the space $(U_h)^3$. Utilizing the properties of Π_h [15], we can derive

$$\sum_{\mathcal{F}\in\mathcal{E}_h^I} h_{\mathcal{F}}||\mathbf{curl}\ \boldsymbol{\Psi} - \Pi_h\mathbf{curl}\ \boldsymbol{\Psi}||_{0,\mathcal{F}}^2 \lesssim h^2\|\boldsymbol{\Psi}\|_{H^1(\mathbf{curl},\Omega)}^2, \tag{53}$$

while using the triangle inequality, inverse inequality, the properties of Π_h [15], and Lemma 4.2, we have

$$\begin{aligned}&\sum_{\mathcal{F}\in\mathcal{E}_h^I} h_{\mathcal{F}}||\Pi_h\mathbf{curl}\ \boldsymbol{\Psi} - \mathbf{curl}\ \widehat{\boldsymbol{\Psi}}_h)||_{0,\mathcal{F}}^2 \lesssim ||\Pi_h\mathbf{curl}\ \boldsymbol{\Psi} - \mathbf{curl}\ \widehat{\boldsymbol{\Psi}}_h)||_{0,\Omega}^2\\ &\lesssim ||\mathbf{curl}\ \boldsymbol{\Psi} - \Pi_h\mathbf{curl}\ \boldsymbol{\Psi}||_{0,\Omega}^2 + ||\mathbf{curl}\ \boldsymbol{\Psi} - \mathbf{curl}\ \widehat{\boldsymbol{\Psi}}_h||_{0,\Omega}^2\\ &\lesssim h^2\|\boldsymbol{\Psi}\|_{H^1(\mathbf{curl},\Omega)}^2.\end{aligned} \tag{54}$$

Combining (53), (54) to (52), we get

$$|b_h(\boldsymbol{E} - \widetilde{\boldsymbol{E}}_h, \boldsymbol{\Psi} - \widehat{\boldsymbol{\Psi}}_h)| \lesssim |||\boldsymbol{E} - \widetilde{\boldsymbol{E}}_h\ |||_h\ (1+\gamma)^{\frac{1}{2}} h\|\boldsymbol{\Psi}\|_{H^1(\mathbf{curl},\Omega)}. \tag{55}$$

Using (48)–(50), (55), and Lemma 4.2, we conclude that

$$\begin{aligned}(\boldsymbol{E}-\widetilde{\boldsymbol{E}}_h,\boldsymbol{w}^0) &= b_h(\boldsymbol{E}-\widetilde{\boldsymbol{E}}_h,\boldsymbol{\Psi}-\widehat{\boldsymbol{\Psi}}_h)+\kappa^2(\boldsymbol{E}-\widetilde{\boldsymbol{E}}_h,\boldsymbol{\Psi}-\widehat{\boldsymbol{\Psi}}_h)\\ &\quad -\mathbf{i}\kappa\lambda\langle(\boldsymbol{E}-\widetilde{\boldsymbol{E}}_h)_T,(\boldsymbol{\Psi}-\widehat{\boldsymbol{\Psi}}_h)_T\rangle_{\partial\Omega}\\ &\lesssim |||\boldsymbol{E}-\widetilde{\boldsymbol{E}}_h|||_h\,(1+\gamma)^{\frac{1}{2}}h\|\boldsymbol{\Psi}\|_{H^1(\mathbf{curl},\Omega)}\\ &\quad +(\kappa^2h^2\|\boldsymbol{E}-\widetilde{\boldsymbol{E}}_h\|_{0,\Omega}+\kappa h^{\frac{3}{2}}\|(\boldsymbol{E}-\widetilde{\boldsymbol{E}}_h\|_{0,\partial\Omega})\|\boldsymbol{\Psi}\|_{2,\Omega}\\ &\lesssim C_{\kappa h}(1+\gamma)^{\frac{1}{2}}h\,|||\,\boldsymbol{E}-\widetilde{\boldsymbol{E}}_h\,|||_h\,\|\boldsymbol{w}^0\|_{0,\Omega}\\ &\quad +(h^2\,|||\,\boldsymbol{E}-\widetilde{\boldsymbol{E}}_h\,|||_h+h^{\frac{3}{2}}\|(\boldsymbol{E}-\widetilde{\boldsymbol{E}}_h)_T\|_{0,\partial\Omega})\|\mathbf{curl}\,\boldsymbol{\Phi}_h^c\|_{0,\Omega}.\end{aligned}\tag{56}$$

From the orthogonality of $\boldsymbol{w}^0$ and ∇r_h^0, by adding and subtracting $\boldsymbol{\Phi}_h+\boldsymbol{E}+\boldsymbol{w}_h^0$, we may derive the following relation:

$$\|\boldsymbol{w}^0\|_{0,\Omega}^2=(\boldsymbol{E}-\widehat{\boldsymbol{E}}_h,\boldsymbol{w}^0)-(\boldsymbol{\Phi}_h-\boldsymbol{\Phi}_h^c,\boldsymbol{w}^0)-(\boldsymbol{w}_h^0-\boldsymbol{w}^0,\boldsymbol{w}^0)-(\boldsymbol{E}-\widetilde{\boldsymbol{E}}_h,\boldsymbol{w}^0),$$

which, together with (56) and Young's inequality, gives

$$\begin{aligned}&\|\boldsymbol{w}^0\|_{0,\Omega}^2\lesssim\|\boldsymbol{E}-\widehat{\boldsymbol{E}}_h\|_{0,\Omega}^2+\|\boldsymbol{\Phi}_h-\boldsymbol{\Phi}_h^c\|_{0,\Omega}^2+\|\boldsymbol{w}_h^0-\boldsymbol{w}^0\|_{0,\Omega}^2\\ &+C_{\kappa h}(1+\gamma)h^2\,|||\,\boldsymbol{E}-\widetilde{\boldsymbol{E}}_h|||_h^2+h\|(\boldsymbol{E}-\widetilde{\boldsymbol{E}}_h)_T\|_{0,\partial\Omega}^2+h^2\|\mathbf{curl}\,\boldsymbol{\Phi}_h^c\|_{0,\Omega}^2.\end{aligned}$$

By (29), (39), (41), and Theorem 4.3, we have

$$\begin{aligned}\|\boldsymbol{w}^0\|_{0,\Omega}&\lesssim\|\boldsymbol{E}-\widehat{\boldsymbol{E}}_h\|_{0,\Omega}+h^{\frac{1}{2}}\|(\boldsymbol{\Phi}_h)_T\|_{0,\partial\Omega}+h\|\mathbf{curl}\,\boldsymbol{\Phi}_h^c\|_{0,\Omega}\\ &\quad+C_{\kappa h}(1+\gamma)^{\frac{1}{2}}h\,|||\,\boldsymbol{E}-\widehat{\boldsymbol{E}}_h\,|||_h+h^{\frac{1}{2}}\|(\boldsymbol{E}-\widetilde{\boldsymbol{E}}_h)_T\|_{0,\partial\Omega}.\end{aligned}\tag{57}$$

While using the triangle inequality, we get

$$h^{\frac{1}{2}}\|(\boldsymbol{\Phi}_h)_T\|_{0,\partial\Omega}\le h^{\frac{1}{2}}(\|(\boldsymbol{E}-\widetilde{\boldsymbol{E}}_h)_T\|_{0,\partial\Omega}+\|(\boldsymbol{E}-\widehat{\boldsymbol{E}}_h)_T\|_{0,\partial\Omega}),$$

and from (39) and (31), we have

$$\begin{aligned}&h\|\mathbf{curl}\,\boldsymbol{\Phi}_h^c\|_{0,\Omega}\le h\|\mathbf{curl}\,(\boldsymbol{\Phi}_h-\boldsymbol{\Phi}_h^c)\|_{0,\Omega}+h\|\mathbf{curl}\,\boldsymbol{\Phi}_h\|_{0,\Omega}\\ &\lesssim h^{\frac{1}{2}}\|(\boldsymbol{\Phi}_h)_T\|_{0,\partial\Omega}+h\,|||\,\boldsymbol{E}-\widehat{\boldsymbol{E}}_h|||_h\\ &\lesssim h^{\frac{1}{2}}(\|(\boldsymbol{E}-\widetilde{\boldsymbol{E}}_h)_T\|_{0,\partial\Omega}+\|(\boldsymbol{E}-\widehat{\boldsymbol{E}}_h)_T\|_{0,\partial\Omega})+h\,|||\,\boldsymbol{E}-\widehat{\boldsymbol{E}}_h\,|||_h\,.\end{aligned}$$

Inserting above two inequalities into (57), we may derive

$$\begin{aligned}\|\boldsymbol{w}^0\|_{0,\Omega}&\lesssim h^{\frac{1}{2}}\|(\boldsymbol{E}-\widetilde{\boldsymbol{E}}_h)_T\|_{0,\partial\Omega}+\|\boldsymbol{E}-\widehat{\boldsymbol{E}}_h\|_{0,\Omega}+h^{\frac{1}{2}}\|(\boldsymbol{E}-\widehat{\boldsymbol{E}}_h)_T\|_{0,\partial\Omega}\\ &\quad+C_{\kappa h}(1+\gamma)^{\frac{1}{2}}h\,|||\,\boldsymbol{E}-\widehat{\boldsymbol{E}}_h\,|||_h\,.\end{aligned}\tag{58}$$

By adding and subtracting $\widehat{\boldsymbol{E}}_h+\Phi_h^c$, using (42) and (40), we have

$$\begin{aligned}\|\boldsymbol{E}-\widetilde{\boldsymbol{E}}_h\|_{0,\Omega}^2&=(\boldsymbol{E}-\widetilde{\boldsymbol{E}}_h,\boldsymbol{E}-\widehat{\boldsymbol{E}}_h)-(\boldsymbol{E}-\widetilde{\boldsymbol{E}}_h,\boldsymbol{\Phi}_h-\boldsymbol{\Phi}_h^c)\\ &\quad-(\boldsymbol{E}-\widetilde{\boldsymbol{E}}_h,\boldsymbol{w}_h^0-\boldsymbol{w}^0)-(\boldsymbol{E}-\widetilde{\boldsymbol{E}}_h,\boldsymbol{w}^0).\end{aligned}$$

Hence,

$$\begin{aligned}\|\boldsymbol{E}-\widetilde{\boldsymbol{E}}_h\|_{0,\Omega} &\lesssim \|\boldsymbol{E}-\widehat{\boldsymbol{E}}_h\|_{0,\Omega}+\|\boldsymbol{\Phi}_h-\boldsymbol{\Phi}_h^c\|_{0,\Omega}+\|\boldsymbol{w}_h^0-\boldsymbol{w}^0\|_{0,\Omega}+\|\boldsymbol{w}^0\|_{0,\Omega}\\ &\lesssim h^{\frac{1}{2}}\|(\boldsymbol{E}-\widetilde{\boldsymbol{E}}_h)_T\|_{0,\partial\Omega}+\|\boldsymbol{E}-\widehat{\boldsymbol{E}}_h\|_{0,\Omega}+h^{\frac{1}{2}}\|(\boldsymbol{E}-\widehat{\boldsymbol{E}}_h)_T\|_{0,\partial\Omega}\\ &\quad +C_{\kappa h}(1+\gamma)^{\frac{1}{2}}h\,|||\,\boldsymbol{E}-\widehat{\boldsymbol{E}}_h|||_h.\end{aligned}$$

This completes the proof of the lemma. □

Next we consider the term $\|(\boldsymbol{E}-\widetilde{\boldsymbol{E}}_h)_T\|_{0,\partial\Omega}$. Note that (29) gives $\|(\boldsymbol{E}-\widetilde{\boldsymbol{E}}_h)_T\|_{0,\partial\Omega}=O(h)$ which, together with (38), implies that $\|\boldsymbol{E}-\widetilde{\boldsymbol{E}}_h\|_{0,\Omega}=O(h^{\frac{3}{2}})$. We can see that half a order of h is lost. In the following, we will improve the error estimate of $\|\boldsymbol{E}-\widetilde{\boldsymbol{E}}_h\|_{0,\Omega}$ through a better estimation for $\|(\boldsymbol{E}-\widetilde{\boldsymbol{E}}_h)_T\|_{0,\partial\Omega}$.

For $\boldsymbol{\Phi}_h=\widetilde{\boldsymbol{E}}_h-\widehat{\boldsymbol{E}}_h\in\boldsymbol{V}_h$, according to Lemma 4.3(ii), we have the following decompositions:

$$\boldsymbol{\Phi}_h=\nabla r+\boldsymbol{w}=\nabla r_h+\boldsymbol{w}_h, \tag{59}$$

where $r\in H^1(\Omega)$, $r_h\in U_h$, $\boldsymbol{w}\in\boldsymbol{H}^1(\Omega)$, and $\boldsymbol{w}_h\in\boldsymbol{V}_h$, $\boldsymbol{w}$ are divergence free in Ω, $\boldsymbol{w}\cdot\boldsymbol{\nu}=0$ on $\partial\Omega$, and there also holds

$$\|\boldsymbol{w}-\boldsymbol{w}_h\|_{0,\Omega}\lesssim h\|\mathbf{curl}\,\boldsymbol{\Phi}_h\|_{0,\Omega}\lesssim h\,|||\,\boldsymbol{E}-\widehat{\boldsymbol{E}}_h|||_h, \tag{60}$$

where we have used (31) to derive the last inequality. The following lemma gives a relationship between $\|(\boldsymbol{E}-\widetilde{\boldsymbol{E}}_h)_T\|_{0,\partial\Omega}$ and $\|\boldsymbol{w}\|_{0,\Omega}$.

Lemma 4.5

$$\begin{aligned}\|(\boldsymbol{E}-\widetilde{\boldsymbol{E}}_h)_T\|_{0,\partial\Omega} &\lesssim \|(\boldsymbol{E}-\widehat{\boldsymbol{E}}_h)_T\|_{0,\partial\Omega}+\kappa^{\frac{1}{2}}\|\boldsymbol{E}-\widehat{\boldsymbol{E}}_h\|_{0,\Omega}\\ &\quad +C_{\kappa h}(h^{-\frac{1}{2}}\|\boldsymbol{w}\|_{0,\Omega}+h^{\frac{1}{2}}\,|||\,\boldsymbol{E}-\widehat{\boldsymbol{E}}_h|||_h).\end{aligned}$$

Proof Denote by

$$d(\boldsymbol{v},\boldsymbol{w}):=\kappa^2(\boldsymbol{v},\boldsymbol{w})-\mathbf{i}\kappa\lambda\langle\boldsymbol{v}_T,\boldsymbol{w}_T\rangle_{\partial\Omega}.$$

Since $b_h(\boldsymbol{E}-\widetilde{\boldsymbol{E}}_h,\nabla r_h)=0$, from (22), we have

$$d(\boldsymbol{E}-\widetilde{\boldsymbol{E}}_h,\nabla r_h)=\widehat{a}_h(\boldsymbol{E}-\widetilde{\boldsymbol{E}}_h,\nabla r_h)=0,$$

which implies

$$d(\boldsymbol{E}-\widetilde{\boldsymbol{E}}_h,\boldsymbol{E}-\widetilde{\boldsymbol{E}}_h)=d(\boldsymbol{E}-\widetilde{\boldsymbol{E}}_h,\boldsymbol{E}-\widehat{\boldsymbol{E}}_h-\boldsymbol{w}_h)$$

and hence from the Cauchy's inequality

$$|d(\boldsymbol{E}-\widetilde{\boldsymbol{E}}_h,\boldsymbol{E}-\widetilde{\boldsymbol{E}}_h)|\lesssim|d(\boldsymbol{E}-\widehat{\boldsymbol{E}}_h-\boldsymbol{w}_h,\boldsymbol{E}-\widehat{\boldsymbol{E}}_h-\boldsymbol{w}_h)|$$

which gives

$$\begin{aligned}\kappa\lambda\|(\boldsymbol{E}-\widetilde{\boldsymbol{E}}_h)_T\|_{0,\partial\Omega}^2 &\le \kappa\lambda\|(\boldsymbol{E}-\widehat{\boldsymbol{E}}_h)_T\|_{0,\partial\Omega}^2+\kappa\lambda\|(\boldsymbol{w}_h)_T\|_{0,\partial\Omega}^2\\ &\quad +\kappa^2\|\boldsymbol{E}-\widehat{\boldsymbol{E}}_h\|_{0,\Omega}^2+\kappa^2\|\boldsymbol{w}_h\|_{0,\Omega}^2\end{aligned}$$

Then the proof of the lemma follows by noting $\|(\boldsymbol{w}_h)_T\|_{0,\partial\Omega} \lesssim h^{-\frac{1}{2}}\|\boldsymbol{w}_h\|_{0,\Omega}$, using (60) and triangle inequality. □

Now we give an estimate for $\|\boldsymbol{w}\|_{0,\Omega}$.

Lemma 4.6 *For the divergence-free term* $\boldsymbol{w}$ *in the decomposition* (59)*, it holds*

$$\|\boldsymbol{w}\|_{0,\Omega} \lesssim \|\boldsymbol{E}-\widehat{\boldsymbol{E}}_h\|_{0,\Omega} + C_{\kappa h}(1+\gamma)^{\frac{1}{2}}h \,|||\, \boldsymbol{E}-\widehat{\boldsymbol{E}}_h \,|||_h + h^{\frac{1}{2}}\|(\boldsymbol{E}-\widehat{\boldsymbol{E}}_h)_T\|_{0,\partial\Omega}. \quad (61)$$

Proof We utilize the duality argument to estimate $\|\boldsymbol{w}\|_{0,\Omega}$, first we begin by introducing the dual problem which is similar to (43)–(44):

$$\mathbf{curl}\,\mathbf{curl}\,\mathbf{z} + \kappa^2\mathbf{z} = \boldsymbol{w} \quad \text{in } \Omega, \quad (62)$$

$$\mathbf{curl}\,\mathbf{z}\times\boldsymbol{\nu} + \mathbf{i}\kappa\lambda\mathbf{z}_T = 0 \quad \text{on } \partial\Omega, \quad (63)$$

Similar to (48) and (49), noting that $\boldsymbol{w}\cdot\boldsymbol{\nu} = 0$ on $\partial\Omega$ and using Theorem 2.1 in [13], we have the following regularity estimates for the above problem:

$$\kappa\|\mathbf{z}\|_{1,\Omega} + \|\mathbf{curl}\,\mathbf{z}\|_{1,\Omega} \lesssim \|\boldsymbol{w}\|_{0,\Omega}, \quad (64)$$

$$\|\mathbf{z}\|_{2,\Omega} \lesssim \|\boldsymbol{w}\|_{0,\Omega} + \kappa^{-2}\|\boldsymbol{w}\|_{1,\Omega} \lesssim \|\boldsymbol{w}\|_{0,\Omega} + \kappa^{-2}\|\,\mathbf{curl}\;\boldsymbol{\Phi}_h\|_{0,\Omega}. \quad (65)$$

Similar to (50)–(56), we may deduce that

$$\begin{aligned}(\boldsymbol{E}-\widetilde{\boldsymbol{E}}_h, \boldsymbol{w}) &= \widehat{a}_h(\boldsymbol{E}-\widetilde{\boldsymbol{E}}_h, \mathbf{z}-\pi_N\mathbf{z})\\ &\lesssim C_{\kappa h}(1+\gamma)^{\frac{1}{2}}h \,|||\, \boldsymbol{E}-\widetilde{\boldsymbol{E}}_h \,|||_h \|\boldsymbol{w}\|_{0,\Omega}\\ &\quad + (h^2 \,|||\, \boldsymbol{E}-\widetilde{\boldsymbol{E}}_h \,|||_h + h^{\frac{3}{2}}\|(\boldsymbol{E}-\widetilde{\boldsymbol{E}}_h)_T\|_{0,\partial\Omega})\|\mathbf{curl}\,\boldsymbol{\Phi}_h\|_{0,\Omega}.\end{aligned}$$

Use (29), (31), and Lemma 4.5 to get

$$\begin{aligned}(\boldsymbol{E}-\widetilde{\boldsymbol{E}}_h, \boldsymbol{w}) &\lesssim C_{\kappa h}(1+\gamma)^{\frac{1}{2}}h \,|||\, \boldsymbol{E}-\widehat{\boldsymbol{E}}_h \,|||_h \|\boldsymbol{w}\|_{0,\Omega}\\ &\quad + C_{\kappa h}(h^2 \,|||\, \boldsymbol{E}-\widehat{\boldsymbol{E}}_h \,|||_h + h\|\boldsymbol{w}\|_{0,\Omega}) \,|||\, \boldsymbol{E}-\widehat{\boldsymbol{E}}_h \,|||_h\\ &\quad + (\|(\boldsymbol{E}-\widehat{\boldsymbol{E}}_h)_T\|_{0,\partial\Omega} + \kappa^{\frac{1}{2}}\|\boldsymbol{E}-\widehat{\boldsymbol{E}}_h\|_{0,\Omega})h^{\frac{3}{2}} \,|||\, \boldsymbol{E}-\widehat{\boldsymbol{E}}_h \,|||_h. \quad (66)\end{aligned}$$

Since $\|\boldsymbol{w}\|^2_{0,\Omega} = (\boldsymbol{\Phi}_h, \boldsymbol{w}) = (\boldsymbol{E}-\widehat{\boldsymbol{E}}_h, \boldsymbol{w}) - (\boldsymbol{E}-\widetilde{\boldsymbol{E}}_h, \boldsymbol{w})$, we have from (66) and the Young's inequality that

$$\|\boldsymbol{w}\|^2_{0,\Omega} \lesssim \|\boldsymbol{E}-\widehat{\boldsymbol{E}}_h\|^2_{0,\Omega} + C_{\kappa h}(1+\gamma)h^2 \,|||\, \boldsymbol{E}-\widehat{\boldsymbol{E}}_h|||^2_h + h\|(\boldsymbol{E}-\widehat{\boldsymbol{E}}_h)_T\|^2_{0,\partial\Omega}.$$

This completes the proof of the lemma. □

By combining Lemmas 4.5 and 4.6, we obtain the following estimate for $\|(\boldsymbol{E}-\widetilde{\boldsymbol{E}}_h)_T\|_{0,\partial\Omega}$.

Lemma 4.7 *Let* $\widetilde{\boldsymbol{E}}_h$ *be the solution of* (22)*, it holds*

$$\begin{aligned}\|(\boldsymbol{E}-\widetilde{\boldsymbol{E}}_h)_T\|_{0,\partial\Omega} &\lesssim C_{\kappa h}(\|(\boldsymbol{E}-\widehat{\boldsymbol{E}}_h)_T\|_{0,\partial\Omega} + h^{-\frac{1}{2}}\|\boldsymbol{E}-\widehat{\boldsymbol{E}}_h\|_{0,\Omega}\\ &\quad + (1+\gamma)^{\frac{1}{2}}h^{\frac{1}{2}} \,|||\, \boldsymbol{E}-\widehat{\boldsymbol{E}}_h|||_h). \quad (67)\end{aligned}$$

Finally we may get the error estimate of $\|\boldsymbol{E}-\widetilde{\boldsymbol{E}}_h\|_{0,\Omega}$ by combining Lemmas 4.4, 4.7, and 4.2.

Theorem 4.4 *Let $\widetilde{\boldsymbol{E}}_h$ be the solution of* (22)*, then the following estimate holds:*

$$\|\boldsymbol{E} - \widetilde{\boldsymbol{E}}_h\|_{0,\Omega} \lesssim C_{\kappa h}(1+\gamma)h^2\|\boldsymbol{E}\|_{2,\Omega}. \tag{68}$$

Proof It follows from Lemmas 4.4 and 4.7 that

$$\|\boldsymbol{E} - \widetilde{\boldsymbol{E}}_h\|_{0,\Omega} \lesssim C_{\kappa h}(h^{\frac{1}{2}}\|(\boldsymbol{E} - \widehat{\boldsymbol{E}}_h)_T\|_{0,\partial\Omega} + \|\boldsymbol{E} - \widehat{\boldsymbol{E}}_h\|_{0,\Omega}$$
$$+(1+\gamma)^{\frac{1}{2}}h \, ||| \, \boldsymbol{E} - \widehat{\boldsymbol{E}}_h |||_h).$$

Then the proof of the theorem follows by using Lemma 4.2. □

Remark 2 The construction of $\boldsymbol{H}(\mathbf{curl}, \Omega)$-elliptic projection (22) in this paper is slightly different from the ones in [7, 18] which is due to the fact that the error estimates in the above papers are based on different norms. For the Helmholtz case in [18], the author derived the $\|\cdot\|_h$-norm error estimate (4.18) in Theorem 4.4, which is defined as $\|\cdot\|_h := (|v|^2_{1,\Omega} + J(v,v))^{1/2}$. Hence, the definition of elliptic projection (4.2) in [18] does not involve an $L^2(\Omega)$ term. For the Maxwell case in [7], the error is estimated in the norm $\|\cdot\|_{\mathrm{DG}}$ which is defined in (7), since an L^2 norm is included in (7), the IPDG $\boldsymbol{H}(\mathbf{curl}, \Omega)$-elliptic projection defined in (5.1) in [7] involves an $L^2(\Omega)$ term. In this paper, we give the error estimate in the energy norm, the definition of which can be founded in (5). Hence, an $L^2(\Omega)$ term with the coefficient κ^2 is included in the $\boldsymbol{H}(\mathbf{curl}, \Omega)$-elliptic projection (22) to grantee the coercivity (24).

4.3 Error estimates for the CIP-FEM

In this subsection, we use the stability estimates derived in Theorem 3.1 and the projection error estimates established in the above subsection to give the error estimates for the scheme (9).

The following stability estimates for $\boldsymbol{E}$ from Theorems 4.1–4.2 will be used in the error analysis:

$$\kappa\,\|\boldsymbol{E}\|_{0,\Omega} + \|\boldsymbol{E}\|_{1,\Omega} + \kappa^{-1}\,\|\boldsymbol{E}\|_{2,\Omega} \lesssim M(\boldsymbol{f},\boldsymbol{g}) \tag{69}$$

where $M(\boldsymbol{f},\boldsymbol{g})$ is defined in Theorem 4.2. Recall that from Theorems 4.3 to 4.4, we have the following error bounds for the elliptic projection:

$$|||\,\boldsymbol{E} - \widetilde{\boldsymbol{E}}_h|||_h \lesssim C_{\kappa h}(1+\gamma)^{\frac{1}{2}}\kappa h M(\boldsymbol{f},\boldsymbol{g}),\ \|\boldsymbol{E} - \widetilde{\boldsymbol{E}}_h\|_{0,\Omega} \lesssim C_{\kappa h}(1+\gamma)\kappa h^2 M(\boldsymbol{f},\boldsymbol{g}). \tag{70}$$

Combined with the stability estimates in Theorem 3.1, we can get the following error estimate for our CIP-FEM.

Theorem 4.5 *Let $\boldsymbol{E}_h$ be the CIP-FE solution to* (9)*, we have*

$$|||\,\boldsymbol{E} - \boldsymbol{E}_h|||_h \lesssim C_{\kappa h}(1+\gamma)(\kappa h + C_{\mathrm{stab}}\kappa^3 h^2)M(\boldsymbol{f},\boldsymbol{g}). \tag{71}$$

Proof Denote by $\boldsymbol{\xi}_h := \boldsymbol{E}_h - \widetilde{\boldsymbol{E}}_h$. From (12) and (22), we obtain

$$a_h(\boldsymbol{\xi}_h, \boldsymbol{F}_h) = -2\kappa^2(\boldsymbol{E} - \widetilde{\boldsymbol{E}}_h, \boldsymbol{F}_h) \quad \forall \boldsymbol{F}_h \in \boldsymbol{V}_h. \tag{72}$$

Then making use of Theorem 3.1 and (70), we have

$$|||\boldsymbol{\xi}_h|||_h \lesssim C_{\text{stab}}\kappa^2\|\boldsymbol{E} - \widetilde{\boldsymbol{E}}_h\|_{0,\Omega} \lesssim C_{\text{stab}}C_{\kappa h}(1+\gamma)\kappa^3h^2M(\boldsymbol{f},\boldsymbol{g}).$$

Hence, by (70) and the triangle inequality, we get

$$\begin{aligned}|||\boldsymbol{E} - \boldsymbol{E}_h|||_h &\leq |||\boldsymbol{E} - \widetilde{\boldsymbol{E}}_h\ |||_h + |||\ \boldsymbol{\xi}_h\ |||_h \\ &\lesssim C_{\kappa h}((1+\gamma)^{\frac{1}{2}}\kappa h + C_{\text{stab}}(1+\gamma)\kappa^3h^2)M(\boldsymbol{f},\boldsymbol{g}).\end{aligned}$$

which concludes the proof of the theorem. □

We can improve the stability estimates in Theorem 3.1 and the error estimates in Theorem 4.5 under the condition that κ^3h^2 is small enough by using the so-called stability-error iterative improvement developed in [8].

Theorem 4.6 *Let $\boldsymbol{E}_h$ be the CIP-FE solution to* (9). *Assuming that $\gamma \simeq 1$, then there exists a constant $C_0 > 0$ independent of κ and h such that when $\kappa^3h^2 \leq C_0$ the following stability and error estimates hold:*

$$|||\ \boldsymbol{E}_h|||_h \lesssim M(\boldsymbol{f},\boldsymbol{g}), \tag{73}$$

$$|||\boldsymbol{E} - \boldsymbol{E}_h|||_h \lesssim (\kappa h + \kappa^3h^2)M(\boldsymbol{f},\boldsymbol{g}). \tag{74}$$

Proof Suppose that there exists a constant $\Lambda > 0$ such that the following stability estimate holds:

$$|||\ \boldsymbol{E}_h|||_h \leq \Lambda M(\boldsymbol{f},\boldsymbol{g}), \quad \forall \boldsymbol{f} \in \boldsymbol{L}^2(\Omega) \text{ and } M(\boldsymbol{f},\boldsymbol{g}) < \infty. \tag{75}$$

Then from (72) and (75) with $\boldsymbol{f} = -2\kappa^2(\boldsymbol{E} - \widetilde{\boldsymbol{E}}_h)$, we have for $\boldsymbol{\xi}_h = \boldsymbol{E}_h - \widetilde{\boldsymbol{E}}_h$,

$$\begin{aligned}|||\boldsymbol{\xi}_h|||_h &\lesssim \Lambda M(\kappa^2(\boldsymbol{E} - \widetilde{\boldsymbol{E}}_h), 0) \\ &= \Lambda(\kappa^2\|\boldsymbol{E} - \widetilde{\boldsymbol{E}}_h\|_{0,\Omega} + \|\ \mathbf{curl}(\boldsymbol{E} - \widetilde{\boldsymbol{E}}_h)\|_{0,\Omega} + \|(\boldsymbol{E} - \widetilde{\boldsymbol{E}}_h) \times \boldsymbol{\nu}\|_{1/2,\partial\Omega}).\end{aligned}$$

From (70), we have

$$\kappa^2\|\boldsymbol{E} - \widetilde{\boldsymbol{E}}_h\|_{0,\Omega} + \|\ \mathbf{curl}(\boldsymbol{E} - \widetilde{\boldsymbol{E}}_h)\|_{0,\Omega} \lesssim (\kappa^3h^2 + \kappa h)M(\boldsymbol{f},\boldsymbol{g}).$$

On the other hand, it follows from the trace inequality, the inverse inequality, Lemma 4.2, and (70) that

$$\begin{aligned}&\|(\boldsymbol{E} - \widetilde{\boldsymbol{E}}_h) \times \boldsymbol{\nu}\|_{1/2,\partial\Omega} \leq \|(\boldsymbol{E} - \widehat{\boldsymbol{E}}_h)_T\|_{1/2,\partial\Omega} + \|(\widehat{\boldsymbol{E}}_h - \widetilde{\boldsymbol{E}}_h)_T\|_{1/2,\partial\Omega} \\ &\lesssim \|(\boldsymbol{E} - \widehat{\boldsymbol{E}}_h)_T\|_{1/2,\partial\Omega} + h^{-1}\|\widehat{\boldsymbol{E}}_h - \widetilde{\boldsymbol{E}}_h\|_{0,\Omega} \\ &\lesssim \|(\boldsymbol{E} - \widehat{\boldsymbol{E}}_h)_T\|_{1/2,\partial\Omega} + h^{-1}(\|\widehat{\boldsymbol{E}}_h - \boldsymbol{E}\|_{0,\Omega} + \|\boldsymbol{E} - \widetilde{\boldsymbol{E}}_h\|_{0,\Omega}) \\ &\lesssim \kappa hM(\boldsymbol{f},\boldsymbol{g}).\end{aligned}$$

Therefore, by combining the above three estimates, we have

$$|||\boldsymbol{\xi}_h|||_h \lesssim \Lambda(\kappa h + \kappa^3h^2)M(\boldsymbol{f},\boldsymbol{g}).$$

Then it follows from the above inequality, (70), and the triangle inequality that

$$|||\ \boldsymbol{E} - \boldsymbol{E}_h|||_h \lesssim (\kappa h + \Lambda(\kappa h + \kappa^3h^2))M(\boldsymbol{f},\boldsymbol{g}) \tag{76}$$

which implies that

$$|||\, \boldsymbol{E}_h |||_h \le |||\boldsymbol{E}\, |||_h + |||\, \boldsymbol{E} - \boldsymbol{E}_h |||_h \lesssim (1 + \kappa h + \Lambda(\kappa h + \kappa^3 h^2)) M(\boldsymbol{f}, \boldsymbol{g}). \quad (77)$$

Repeating the above process yields that there exists a constant $\widetilde{C}$ independent of κ and h, and a sequence of positive number Λ_j such that

$$|||\, \boldsymbol{E}_h |||_h \le \Lambda_j M(\boldsymbol{f}, \boldsymbol{g}), \quad (78)$$

with

$$\Lambda_j = \widetilde{C}(1 + \kappa h) + \widetilde{C}(\kappa h + \kappa^3 h^2)\Lambda_{j-1}, \quad j = 1, 2, \ldots.$$

and noting from Theorem 3.1 that $\Lambda_0 \simeq C_{\text{stab}}$. A simple calculation yields that if $\widetilde{C}(\kappa h + \kappa^3 h^2) \le \theta$ for some positive constant $\theta < 1$, then

$$\lim_{j\to\infty} \Lambda_j = \frac{\widetilde{C}(1 + \kappa h)}{1 - \widetilde{C}(\kappa h + \kappa^3 h^2)}, \quad (79)$$

which implies (73). Then (74) follows from (76). This completes the proof of the theorem. □

Remark 3 We would like to mention that similar stability and error estimates of the standard FEM for time-harmonic Maxwell equation are not straightforward as the Helmholtz case in [18]. Recall that the stability and error estimates of the standard FEM in [18] are proved by using Cauchy's convergence test and taking the limit as the penalty parameter tends to zero. In fact, the inequality (6.6) which is derived from Theorem 5.1 in [18] plays an important role for the convergence of u_h^γ. However, the stability estimate of $\boldsymbol{E}_h$ when $\kappa^3 h^2$ is small imposes more strict condition on the right hand side terms $\boldsymbol{f}$ and $\boldsymbol{g}$. Unfortunately, similar result like (6.6) in [18] can not be deduced for the time-harmonic Maxwell case. The stability estimate and convergence analysis of the standard FEM for time-harmonic Maxwell equation need further investigation which constitutes our future work.

5 Numerical results

In this section, we present two numerical examples to demonstrate the convergence property of the CIP-FEM in three dimension. We employ the linear Nédélec edge element of second type on shape regular tetrahedral meshes. Although the theories presented in the above section give the bound on the Galerkin error in terms of the data, we perform the relative error in our numerical experiments for simplicity. The following implementation is based on a MATLAB software package iFEM (cf. [4]).

Example 5.1 We consider the time-harmonic Maxwell problem in a unit cube $\Omega = [0, 1] \times [0, 1] \times [0, 1]$:

$$\begin{aligned} \textbf{curl}\,\textbf{curl}\, \boldsymbol{E} - \kappa^2 \boldsymbol{E} &= \boldsymbol{0} \qquad \text{in } \Omega, \\ \textbf{curl}\, \boldsymbol{E} \times \boldsymbol{\nu} - \mathbf{i}\kappa \boldsymbol{E}_T &= \boldsymbol{g} \qquad \text{on } \partial\Omega. \end{aligned}$$

Here $\boldsymbol{g}$ is chosen such that the exact solution is given by

$$\boldsymbol{E} = (e^{\mathbf{i}\kappa z}, e^{\mathbf{i}\kappa x}, e^{\mathbf{i}\kappa y})^T.$$

In this example, we first verify the stability of our CIP-FEM. In Fig. 1, we plot the following two ratios:

$$\frac{|||\boldsymbol{E}_h|||_h}{|||\boldsymbol{E}|||_h} \text{ and } \frac{|||\boldsymbol{E}_h^{\mathrm{FEM}}|||_h}{|||\boldsymbol{E}|||_h}$$

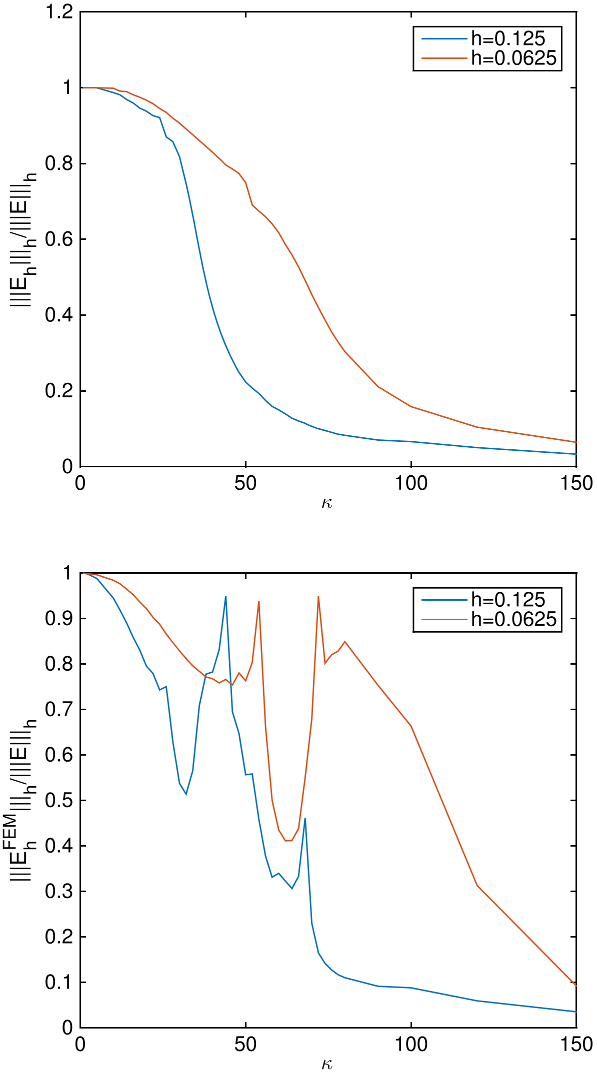

Fig. 1 Left: $\frac{|||\boldsymbol{E}_h|||_h}{|||\boldsymbol{E}|||_h}$ and right: $\frac{|||\boldsymbol{E}_h^{\mathrm{FEM}}|||_h}{|||\boldsymbol{E}|||_h}$ for $\kappa = 1, 2, ...150$ with $h = \frac{1}{8}, \frac{1}{16}$, respectively

for $\kappa = 1, 2, \ldots 150$ with $h = \frac{1}{8}, \frac{1}{16}$ respectively, where $\boldsymbol{E}_h^{\mathrm{FEM}}$ denotes the standard finite element solution and the parameter γ_F in CIP-FEM is chosen as 0.01–0.08i. It can been seen that the ratio $|||\boldsymbol{E}_h|||_h/|||\boldsymbol{E}|||_h$ of CIP-FEM decreased with respect to κ for fixed h while the ratio $|||\boldsymbol{E}_h^{\mathrm{FEM}}|||_h/|||\boldsymbol{E}|||_h$ of standard FEM oscillates with κ, which confirms our theoretical analysis in Theorem 3.1 and indicates that CIP-FEM is more stable than standard FEM. Figure 2 shows the ratio $|||\boldsymbol{E}_h|||_h/|||\boldsymbol{E}|||_h$ of CIP-FEM with respect to the wave number when the mesh condition satisfies $\kappa^3 h^2 = 5$, which is almost a constant as predicted in (73).

The left graph in Fig. 3 displays the relative error of the CIP-FEM with penalty parameter $\gamma_F = 0.1$, $\gamma_F = 0.01 - 0.08\mathbf{i}$, and $\gamma_F = 0.01 + 0.08\mathbf{i}$ respectively and the relative error of the standard edge element solution in the energy norm when the mesh condition is restricted to $\kappa h = 2.5$. It shows that the relative error can not be controlled by κh and increases with κ, which indicates the existence of the pollution error. We would like to mention that the theoretical analysis of CIP-FEM can be extended to the case when $\gamma_{\mathcal{F}}$ is a complex number with positive real part and negative imaginary part; for the case that $\gamma_{\mathcal{F}}$ is a complex number with positive imaginary part, the theoretical analysis in this paper do not hold. It can be seen from the left graph in Fig. 3 that the CIP-FEM with $\gamma_{\mathcal{F}} = 0.01+0.08\mathbf{i}$ performs worse than $\gamma_{\mathcal{F}} = 0.01 - 0.08\mathbf{i}$ and $\gamma_{\mathcal{F}} = 0.1$. Hence, in the following, we will avoid to choose $\gamma_{\mathcal{F}}$ with positive imaginary part. The right graph in Fig. 3 displays the relative error of the CIP-FEM with penalty parameter $\gamma_F = 0.1$ and $\gamma_F = 0.01 - 0.08\mathbf{i}$ based on the mesh condition $\kappa^3 h^2 = 5$. We observe that under this mesh condition, the relative error does not increase with κ and is bounded by $O(\kappa h + \kappa^3 h^2)$ which confirms the error estimate (74).

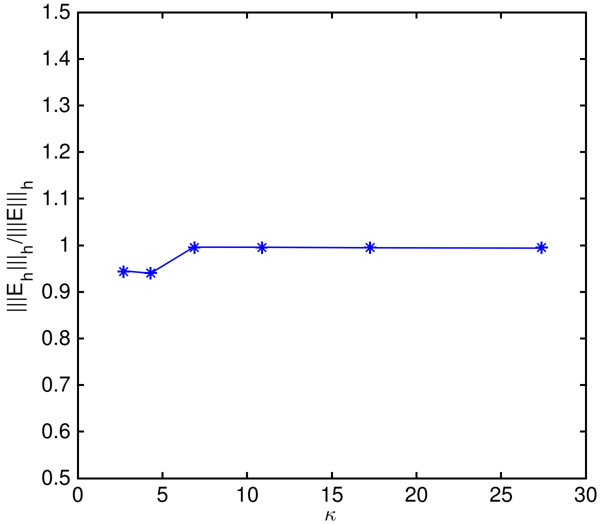

Fig. 2 The ratio $\frac{|||\boldsymbol{E}_h|||_h}{|||\boldsymbol{E}|||_h}$ of CIP-FEM under the mesh condition $\kappa^3 h^2 = 5$

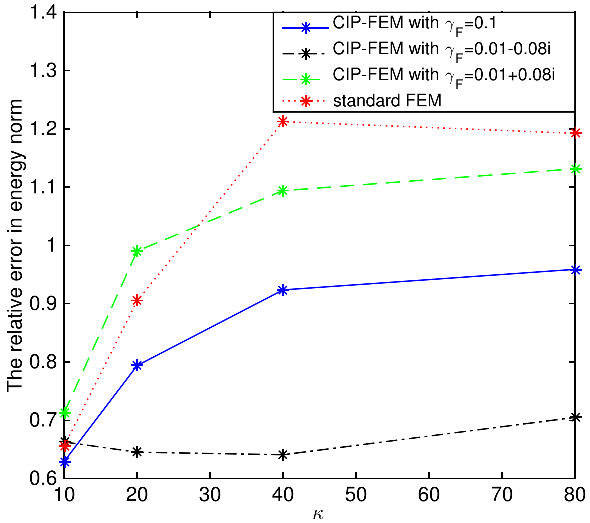

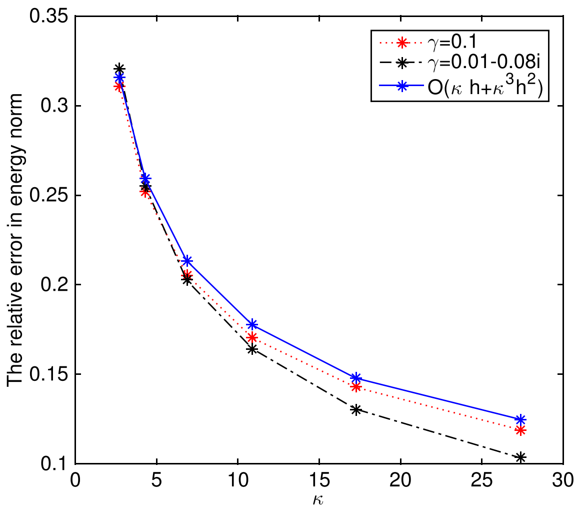

Fig. 3 Left: the relative error of CIP-FEM with three different penalty parameter γ_F and the relative error of edge element solution in the energy norm under the mesh condition $\kappa h = 2.5$. Right: the relative error of CIP-FEM with two different penalty parameter γ_F in the energy norm under the mesh condition $\kappa^3 h^2 = 5$

Another advantage of the CIP-FEM is the flexibility of tuning the penalty parameter γ_F. We may observe from the left graph of Fig. 3 that the CIP-FEM with the penalty parameter $\gamma_F = 0.01 - 0.08\mathbf{i}$ performs better than the case with $\gamma_F = 0.1$ and the standard edge element solution. Although the pollution error has not been eliminated, it is significantly reduced. For more detailed comparison between the

CIP-FEM and standard edge element method, we consider the problem with wave number $\kappa = 32$. In order to compare the phase error of the solutions, we restrict to the line segment $x = 0.5$, $y = 0.5$ and $0 \leq z \leq 1$ and observe the traces of the real part of the first component of the CIP-FEM solution with $\gamma_F = 0.01 - 0.08\mathbf{i}$ and standard edge element solution with mesh sizes $h = 1/16$ and $h = 1/32$, respectively. The traces of the real part of the first component for the exact solution are also plotted in blue line in Fig. 4. On the coarse mesh with $h = 1/16$, the shape of the CIP-FEM solution is roughly the same as the exact solution, while the standard edge element solution has a wrong shape. On the fine mesh with $h = 1/32$, the shape of the CIP-FEM solution is almost the same as the exact solution, but the edge element solution still does not match the exact solution very well. We should note that this "optimal" penalty parameter is chosen from [7]. It is simply chosen from the set $\{0.01(p + q\mathbf{i}), -50 \leq p, q \leq 50\})$ to minimize the relative error in energy norm

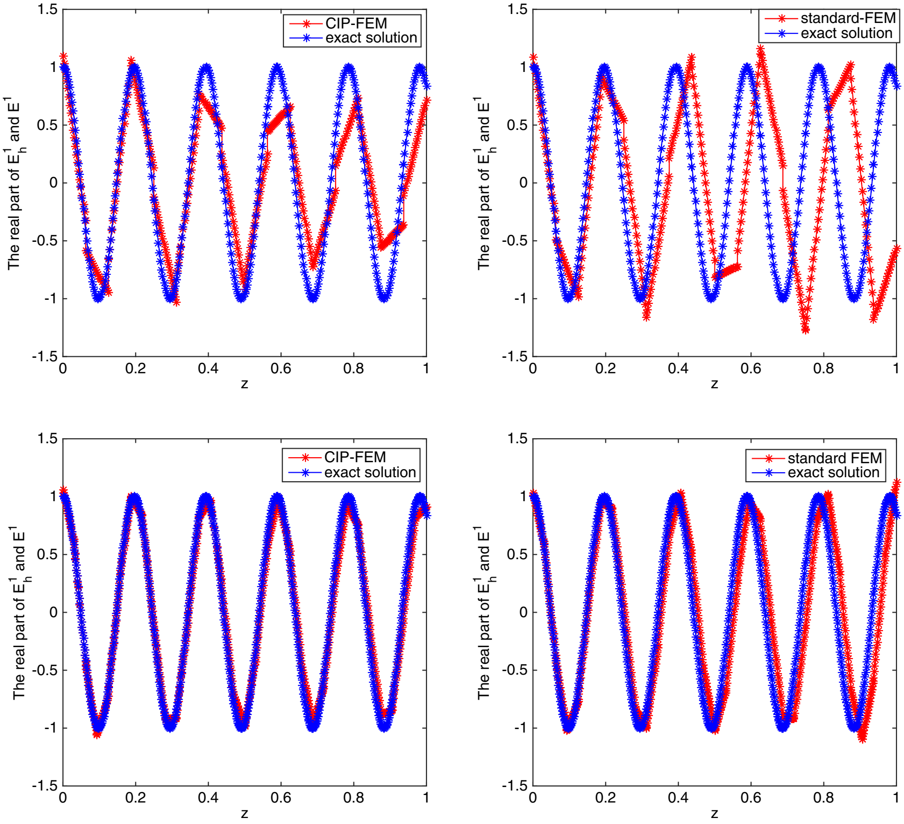

Fig. 4 Left: the traces of the real part of the first component of the CIP-FEM solution with $\gamma_F = 0.01 - 0.08i$ for $\kappa = 32$ with mesh size $h = 1/16$ and $h = 1/32$ respectively. Right: the case for the standard edge element solution

for wave number $\kappa = 20$ and $h = 1/10$. The optimal penalty parameter can also be obtained by the dispersion analysis [2], which is a subject worth of investigation.

Finally, we show the numbers of total degree of freedoms (DOFs) needed for reducing the relative errors in energy norm to 30% for the edge element solution, IPDG solution developed in [7], and our CIP-FEM. It can be seen from Table 1 that our CIP-FEM needs less DOFs than the IPDG method, and much less for large wave number κ than the edge element solution.

Example 5.2 We consider the time-harmonic Maxwell problem with the impedance boundary condition:

$$\begin{aligned} \mathbf{curl}\,\mathbf{curl}\,\boldsymbol{E} - \kappa^2 \boldsymbol{E} &= \qquad \text{in } \Omega, \\ \mathbf{curl}\,\boldsymbol{E} \times \boldsymbol{\nu} - \mathbf{i}\kappa \boldsymbol{E}_T &= \boldsymbol{g} \qquad \text{on } \partial\Omega. \end{aligned}$$

Here $\Omega = [0, 1] \times [0, 1] \times [0, 1]$ is a unit cube, and $\boldsymbol{f}$ and $\boldsymbol{g}$ are chosen such that the exact solution is given by

$$\boldsymbol{E} = (\sin(\kappa y) J_0(\kappa r), \cos(\kappa z) J_0(\kappa r), \mathbf{i}\kappa J_0(\kappa r))^T$$

in polar coordinates, where $r = \sqrt{x^2 + y^2 + z^2}$ and $J_0(z)$ is Bessel function of the first kind. Although we assume that the right-hand side $\boldsymbol{f}$ of the equation (1) is a solenoidal current density, we find that the numerical results are also valid for the case $\mathbf{div}\boldsymbol{f} \neq 0$.

For fixed wave number κ, we first show the relative error in the energy norm with respect to the CIP-FEM and standard edge element solution. The left graph in Fig. 5 displays the relative error of the CIP-FEM solution with $\gamma_F = 0.1$ in the energy norm for $\kappa = 10, 20$, and 30, while the right one shows the relative error for the cases based on the standard edge element method. We find that the relative error of the CIP-FEM stays around 100% while the standard edge element method oscillates around 100% when the mesh size is not small enough for the wave number κ, which confirms the stability property of our theoretical analysis for the CIP-FEM and indicates that the CIP-FEM is more stable than the standard edge element method especially for large wave number κ.

Figure 6 displays the relative error in the energy norm according to different mesh size conditions. The left one shows the relationship between the relative error and the wave number κ under the mesh condition $\kappa h = 2.5$ for the CIP-FEM and standard

Table 1 Numbers of total DOFs needed for 30% relative errors in energy norm for the edge element solution, IPDG solution, and our CIP-FEM

κ	10	20	30	40
FEM	9504	127008	649728	2208384
IPDG	12000	96000	324000	768000
CIP-FEM	8368	62048	204048	477376

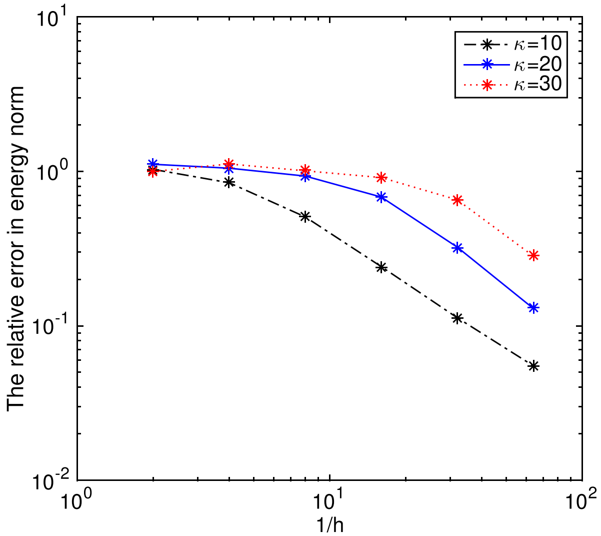

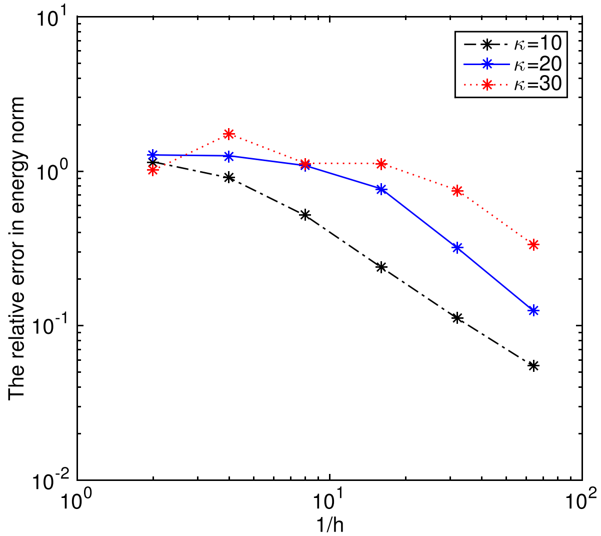

Fig. 5 The relative error of CIP-FEM and edge element solution against $\frac{1}{h}$ in the energy norm for $\kappa = 10, 20, 30$, respectively (left to right)

edge element solutions. We may observe that although both the relative error of CIP-FEM and edge element solution increase with κ, the CIP-FEM performs better than the standard edge element solution. The right graph of Fig. 6 shows the relative error of the CIP-FEM on the mesh condition $\kappa^3 h^2 = 5$, from which we may see that the relative error can be controlled under this mesh condition.

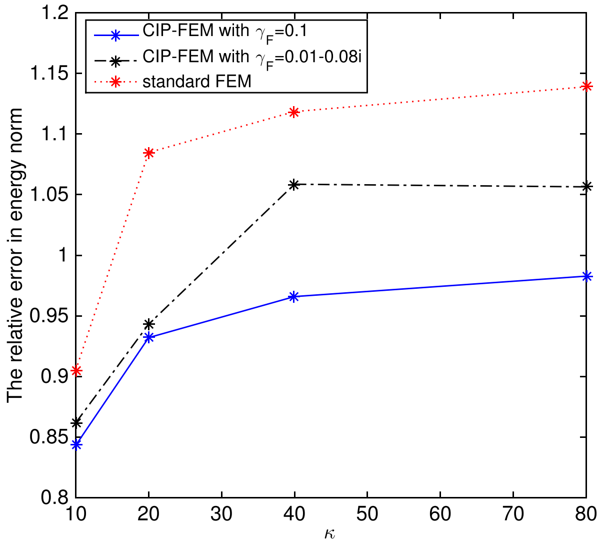

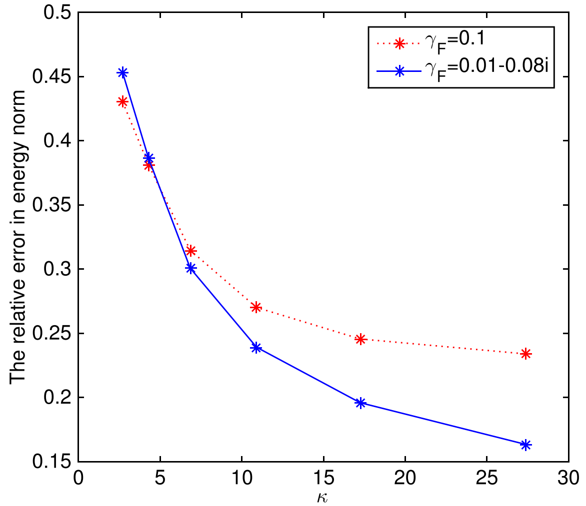

Fig. 6 Left: the relative error of CIP-FEM and edge element solution in the energy norm under the mesh condition $\kappa h = 2.5$. Right: the relative error of CIP-FEM in the energy norm under the mesh condition $\kappa^3 h^2 = 5$

Acknowledgments We thank the editor and the anonymous referees, who meticulously read through the paper and made many helpful suggestions which led to an improved presentation of this paper.

Funding Information We would like to note that the work of Haijun Wu was partially supported by the National Natural Science Foundation of China under grants 11525103 and 91630309 and the work of the Xuejun Xu was supported by National Natural Science Foundation of China (Grant Nos. 11671302 and 11871272).

References

1. Adams, R.: Sobolev Spaces. Academic Press, New York (1975)
2. Ainsworth, M.: Dispersive properties of high order Nédélec/edge element approximation of the time-harmonic Maxwell equations. Philos. Trans. R. Soc. Lond. Ser. A Math. Phys. Eng. Sci. **362**, 471–491 (2004)
3. Brenner, S., Li, F., Sung, L.: A locally divergence-free nonconforming finite element method for the time-harmonic Maxwell equations. Math. Comp. **70**, 573–595 (2007)
4. Chen, L.: IFEM: an integrated finite element methods package in MATLAB, Technical Report, University of California at Irvine (2009)
5. Cuvelier, C., Segal, A., Steenhoven, A.: Finite element methods and Navier-Stokes equations. D. Reidel Publishing Company, Dordrecht (1986)
6. Douglas, J. Jr., Dupont, T.: Interior penalty procedures for elliptic and parabolic Galerkin methods, Lecture Notes in Phys., 58. Springer, Berlin (1976)
7. Feng, X., Wu, H.: An absolutely stable discontinuous Galerkin method for the indefinite time-harmonic Maxwell equations with large wave number. SIAM J. Numer. Anal. **52**, 2356–2380 (2014)
8. Feng, X., Wu, H.: *hp*-discontinuous Galerkin methods for the Helmholtz equation with large wave number. Math. Comp. **80**, 1997–2024 (2011)
9. Hiptmair, R., Moiola, A.: Stability results for the time-harmonic Maxwell equations with impedance boundary conditions. Math. Models Methods Appl. Sci. **21**, 2263–2287 (2011)
10. Hiptmair, R., Moiola, A., Perugia, I.: Error analysis of Trefftz-discontinuous Galerkin methods for the time-harmonic Maxwell equations. Math. Comp. **82**, 247–268 (2013)
11. Houston, P., Perugia, I., Schneebeli, A., Schötzau, D.: Interior penalty method for the indefinite time-harmonic Maxwell equations. Numer. Math. **100**, 485–518 (2005)
12. Houston, P., Perugia, I., Schötzau, D.: Mixed discontinuous Galerkin approximation of the Maxwell operator, SIAM. J. Numer. Anal. **42**, 434–459 (2004)
13. Lu, P., Wang, Y., Xu, X.: Regularity results for the time-harmonic Maxwell equations with impedance boundary condition, submitted, https://arxiv.org/pdf/1804.07856.pdf
14. Melenk, J.M., Sauter, S.: Wavenumber-explicit *hp*-FEM analysis for Maxwell's equations with transparent boundary conditions, arXiv:1803.01619 (2018)
15. Monk, P.: Finite element methods for Maxwell's equations. Oxford University Press, New York (2003)
16. Nicaise, S., Tomezyk, J.: Convergence analysis of a *hp*-finite element approximation of the time-harmonic Maxwell equations with impedance boundary conditions in domains with an analytic boundary, https://hal.archives-ouvertesfr/hal-02063271/ (2019)
17. Perugia, I., Schötzau, D., Monk, P.: Stabilized interior penalty methods for the timeharmonic Maxwell equations. Comput. Methods Appl. Mech. Engrg. **191**, 4675–4697 (2002)
18. Wu, H.: Pre-asymptotic error analysis of CIP-FEM and FEM for Helmholtz equation with high wave number. Part I: Linear version. IMA J. Numer. Anal. **34**, 1266–1288 (2014)
19. Zhong, L., Shu, S., Wittum, G., Xu, J.: Optimal error estimates for nédélec edge elements for time-harmonic Maxwell's equations. J. Comp. Math. **27**, 563–572 (2009)